Recent SQUID Activities in Europe, Part II: Applications

Alex I. Braginski[1] and Gordon B. Donaldson[2]

(1) Forschungszentrum Jülich, GmbH (FZJ), D-52425 Jülich, Germany

(2) Dept. of Physics, University of Strathclyde, Glasgow G4 0NG, Scotland, UK

E-mail: a.braginski@fz-juelich.de; g.b.donaldson@strath.ac.uk

***Abstract* – We present an overview of recent superconducting quantum interference device (SQUID) research and development in Europe. History, theory and fundamental experiments and especially practical SQUIDs and SQUID readout were covered by Part I of this overview. Today, the SQUID itself is a rather mature device, the most sensitive magnetic flux and field detector, which finds use also as an amplifier. The current research and development work concentrates mostly on the more traditional and novel applications presented here. We briefly characterize the evolution and status of the following applications: biomagnetic (mostly medical), radiation and particle detection, geomagnetism and related, nondestructive evaluation of materials and structures (NDE), metrology, and fundamental scientific experiments. Some of these found practical acceptance, while the promise and potential of others remains largely unfulfilled. Of all these, the radiation and particle detectors attract presently the most interest and are in a phase of fast development.**

Received June 30, 2009; accepted July 30, 2009. Reference No. CR12-II; Category 4.

***Keywords* - SQUID, SQUID application, biomagnetism, magnetoencephalography, MEG, magnetocardiography, MCG, liver susceptometry, electromagnetic radiation detector, TES, SQUID readout, NDE, airplane NDE, geophysical surveying, TEM, archeometry, metrology, thermometry, CCC, cryogenic current comparator, SQUIF, pi-junction, gravity wave detection, nanoSQUID, extreme sensor**

I. INTRODUCTION

The very first application of the SQUID was probably its use as a sensitive galvanometer and picovoltmeter, both devices demonstrated by John Clarke in [1,2,3]. Today, applications of SQUIDs as the most sensitive magnetic flux and field detectors and as amplifiers are multiple, but most of the SQUIDs used worldwide are in large multichannel biomagnetic systems, especially those for whole-head functional imaging of the electromagnetic activity of the human brain (magnetoencephalography, abbreviated MEG). A newly emerged application, where rapidly increasing SQUID numbers are used, mostly as amplifiers and in multiplexer circuits, is the readout of large radiation and particle detector arrays, for example in radioastronomy. For other applications rather small SQUID numbers are used in situations where room-temperature devices do not provide the required sensitivity or other desired performance characteristics. This overview is limited only to SQUIDs for analog applications, where the European contribution has been significant. Military applications are not included. We do not discuss the application methodology, *etc*., but take a brief look at suitable SQUID systems and their performance. Comprehensive overviews of all analog applications of SQUIDs can be found in [4].

In this article, we often refer to the material included in Part I of this overview, which concentrates on SQUID devices and is published in the preceding issue of ESNF [5]. We refer to it as "Part I". Here, we assume that this Part I is known to the reader.

II. BIOMAGNETIC APPLICATIONS

A. General

Sensing of minute magnetic fields emitted by living organisms and biological samples has been performed with SQUID sensors almost from their inception. The size limit of this overview does not permit us to overview all such applications, which are presented in [6,7], and also very briefly in [8]. When listing this reference, we provide a hyperlink to a table succinctly characterizing all biomagnetic methods. Here, we briefly describe only these three applications, which have been successfully used in either research or clinical diagnostics, or may have a high potential for saving human lives: MEG, magnetocardiography (MCG) and liver susceptometry. We also comment on the newest biomagnetic method currently under study: the low-field magnetic resonance imaging (LFMRI).

Cohen *et al* first used a SQUID to measure the magnetic field of heart and brain in at the beginning of the 1970s [9,10], and this made both MCG and MEG of interest to a rapidly increasing number of research groups. Initially, these activities and the development of suitable SQUID systems were limited to the US, but by 1985 SQUIDs were developed for and used in biomagnetic measurements also in Europe, especially in Finland (at HUT), Germany (PTB-Berlin), Italy (CNR-Rome) and in the Netherlands (Univ. of Twente). Biomagnetic measurements have been, as a rule, conducted in magnetically shielded rooms (MSR) to minimize external disturbance signals and assure an acceptable signal-to-noise (SNR) ratio for very weak signals. The intensity of human brain signals is typically in the range of only 10^{-13} to 10^{-14} tesla, while the human adult heart signal is relatively stronger, at 10^{-10} to 10^{-11} tesla. The heart signal frequency range extends from nearly zero to a few hundred Hz, while brain signals extend to a few kHz.

B. Magnetoencephalography (MEG)

The need for multichannel systems permitting functional imaging, especially in MEG (but also MCG) became obvious rather early. However, throughout the 1980s the number of channels remained in single digits range (4 to 7), because of technology limitations, also in massive signal and data processing. Probably the first European 4-channel system for brain research was reported on by Ilmoniemi *et al*. in 1984 [11]. It still used rf SQUIDs fabricated by SHE, but about that time the development of planar coupled dc SQUIDs also started in Europe. The Finnish effort was assisted by collaboration with IBM, Yorktown Heights, where the modern planar dc SQUIDs originated [12], and resulted in the transfer of IBM technology to HUT. Indeed, already by 1987 a 7-channel dc SQUID system with first-order gradiometers positioned on a spherical surface of 125-mm radius, a fruit of HUT collaboration with IBM, was in routine use in Finnish brain research [13]. It can be seen as an early precursor of all modern dc SQUID whole-head biomagnetometers for brain studies. The sensor field noise was a very respectable 5 $fT/Hz^{1/2}$.

A milestone on the way to the modern multichannel biomagnetic systems was the first ever 37-channel system developed by Siemens (the "Krenikon") at the beginning of the 1990s, already commented on in Part I [14]. Several such commercial systems were installed

at various clinical centers in Germany and elsewhere in Europe. Also Philips presented soon thereafter a 31-channel commercial system, and another experimental 37-channel system was demonstrated by PTB-Berlin. All these systems used a nearly planar array of SQUID sensors, a compromise between MEG and MCG requirements. This compromise wasn't really acceptable for brain research, and by 1992-1993 the first European whole-cortex system with 122 channels at 61 locations was developed by HUT and the spun-off Neuromag Ltd [15]. Figure 1 shows schematically the cryostat with the helmet-shaped tip covering the whole cortex, with the main inside components on the left side and the 1st order planar gradiometers on the right side. At each measuring point there is a pair of such gradiometers orthogonal to each other, and an additional magnetometer. This sensor configuration at each measuring point combines the focal sensitivity of planar gradiometers, which measure $\partial B_z/\partial x$ and $\partial B_z/\partial y$, and the less directional sensitivity of the magnetometer measuring the normal component B_z [16]. The magnetometer intrinsic noise is on the order of 1 $fTHz^{-1/2}$; other technical details can be found in [15]. The gradiometers were also described in Part I. Also described there was the adaptive noise cancellation technique with positive feedback [17,18], which made it possible to place all the electronics, including preamplifiers, outside of the MSR. The quantitative performance characteristics of the Elekta Neuromag® sensor array are described in [19].

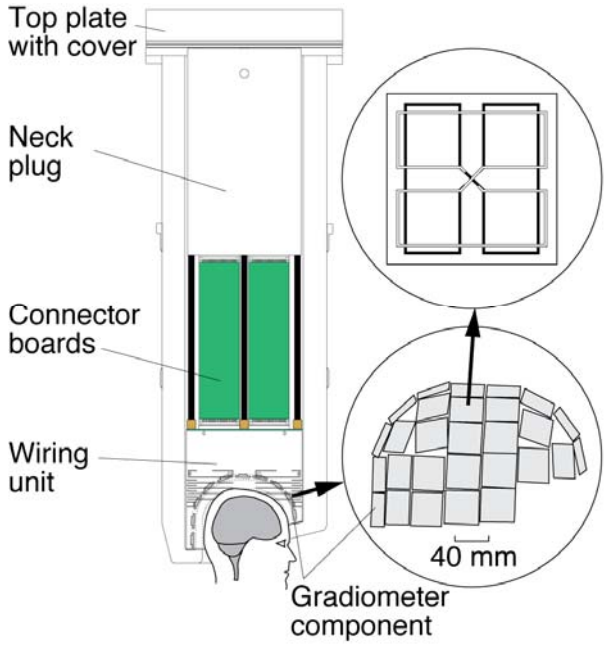

Fig. 1. The first whole-cortex cryostat for MEG (left) and the planar gradiometer arrangement (right) [15]. Schematic representation of the integrated planar gradiometer pair measuring the orthogonal tangential derivatives $\partial B_z/\partial x$ and $\partial B_z/\partial y$ of the magnetic field B_z (Courtesy of A. Ahonen, Elekta-Neuromag).

Just about the time of introduction of the HUT/Neuromag prototype, Siemens and a little later Philips too withdrew from the market and abandoned further MEG system development, because of "insufficient market prospects". The field was left to small enterprises. Today, MEG is an accepted research tool, with large, mostly whole-cortex systems equipped with up to 500 channels. Elekta Neuromag® became the dominant European commercial supplier of MEG systems [20]. Figure 2 shows their modern system operable in both supine and upright (patient sitting) configuration and capable of detailed functional imaging of the cortex. It

includes 306 SQUID channels and 64 (or 124) auxiliary EEG (electroencephalography) channels. At present, the main research application of such systems is in neurology and psychology. Well over 100 commercial systems by various manufacturers are installed worldwide, essentially for research purposes.

In this decade, experimental systems with vectorially configured sensors (measuring B_x, B_y, and B_z at each point location on the measurement grid) were also developed in Europe. One system was developed and operates at PTB-Berlin [21], another, constructed by AtB [22], is located at the Biomagnetic Center Jena. Both these systems use essentially flat bottom dewars. They serve for various neurological and other biomagnetic investigations (rather than conventional MEG as such), and for evaluation of localization methodologies [23]. An example of neurological use is the registration of magnetic fields generated by infra-slow brain activity, a method known as the dc MEG [24]. Methodology studies showed superior source localization accuracy and net information gain when compared with single field component measurements [25,26].

Three-dimensional (3D) localization of local activity centers in the brain requires solving the inverse problem in three dimensions, which is ill-posed, and thus can have only an approximate solution based on assumed boundary conditions, simultaneous electroencephalography (EEG) data, and appropriate additional anatomical information. This is usually obtained via the superposition of anatomic images separately obtained by magnetic resonance imaging (MRI) on functional images from MEG. Although special markers positioned on the subject's head are used, but the superposition procedure is unavoidably leading to localization inaccuracy on the order of 1 cm, which also increases with depth (distance from SQUID sensor). A detailed discussion of the inverse problem, also in application to MEG, is given in [27].

Wide diagnostic use of MEG systems was expected, mainly as tools for pre-surgical functional mapping, for example, of epileptic foci. Unfortunately, such hopes have not materialized thus far[1]. Surgeons having MEG equipment at their disposal find it quite helpful, but others, not having it, do not deem it to be absolutely necessary. Other, new diagnostic applications have not developed so far, although efforts in this direction continue[2]. Consequently, the market for such large and expensive systems remains rather small.

Both in Europe and in the US, there is also research interest in MEG of fetuses and infants (perinatal MEG) [8], although that research is still in its initial phase.

Currently, renewed interest in MEG focuses on the possibility of employing the same SQUID sensor array for both functional and anatomical visualization, which could dramatically improve localization accuracy. The latter possibility is offered by the very low-field nuclear magnetic resonance imaging (LFMRI) pursued actively at Berkeley [28], at the Los Alamos National Laboratory (LANL), at PTB-Berlin, and most recently under a European project involving several laboratories [29]. The LANL group have already demonstrated an experimental 7-channel system capable of "parallel" MRI and MEG, with data acquisition performed sequentially in time for the same subject (patient) [30]. Such hybrid MRI-MEG systems might still become of broader clinical interest.

[1] In spite of the insurance coverage in the United States.

[2] It is encouraging to note that at this writing MEG systems are being installed in two Italian private clinics for unspecified diagnostic rather than research use (M. Russo, Istituto di Cibernetica "E.Caianiello" CNR, Naples, Italy; private communication, June 2009)

Fig. 2. An Elekta Neuromag MEG system (signal and data processing equipment not shown), operable in supine and upright patient position within an MSR (Courtesy of Elekta Neuromag).

C. Magnetocardiography, Magnetic Functional Imaging

Magnetocardiography and the magnetic functional imaging (MFI) of the heart employ the same underlying principles as MEG, including the algorithms necessary for visualization and approximate functional localization. In contrast to MEG, it could be valuable mostly for fast, noninvasive diagnostics and screening of population, rather than in-depth heart research.

The number of sensing channels in dedicated MCG systems is usually lower than in MEG, and remains in the range of 9 to about 50, in part to cap the cost of such equipment. For simultaneous imaging of the whole heart at least 36 channels are required. At this juncture, the only commercial system really suitable for MFI of human heart is that developed by BMDSys, a small German company [31]. Their system Apollo CXS has 55 sensing channels, most technical details are not available. In the US, a 9-channel system claimed to operate successfully without MSR has been developed and marketed by CardioMag Imaging (CMI), earlier in this decade [32]. Operation without MSR is thought possible, because cardiac signals are stronger than brain signals. A few rather successful clinical studies performed using CMI systems were published, for example [33,34], but so far have not produced any breakthrough in clinical acceptance worldwide. Further clinical studies continue, but only at few locations worldwide.

Relatively simple MCG systems involving a few channels have great potential usefulness in perinatal cardiological diagnostics and management of fetuses and infants, even if not suitable for MFI of the whole heart. For example, in the case of fetuses, details of the heart rhythm can be easily monitored even during the period of *vernix caseosa*, from approximately 28 to 33 week of gestation, when electrocardiographic recording is not possible [7]. It appears that interest in perinatal heart diagnostics using SQUIDs is growing both in Europe and in the US [35].

We believe noninvasive heart diagnostics using MFI has a very high potential for saving human lives at a cost significantly lower than other noninvasive imaging techniques, such as

high-field (conventional) MRI. Magnetic imaging is also much more comfortable to the subject than MRI. The MFI method is in principle suitable for diagnosis of a wide range of ventricular/coronary heart diseases (CVD, CHD) and of arrhythmia problems. Unfortunately, most clinical studies published to date had insufficient statistical value or suffered from substandard performance of the equipment, especially when operating without magnetic shielding. The future will show whether ongoing clinical MFI studies will result in a real breakthrough in clinical acceptance or not. The method will be broadly used only when reimbursed by insurance companies, which is not the case at present. Even if MFI doesn't become broadly accepted, it is likely that an MCG niche in perinatal cardiology will eventually be firmly established.

D. Liver Susceptometry

The liver disease diagnostics by magnetic susceptometry does not involve imaging [36]. It consists of integral quantitative assessment of excess iron stored in the liver. The liver area is subjected to an inhomogeneous magnetic field (in low mT range) of superconducting coils, as shown schematically in Figure 3(a). During the susceptibility measurement, the patient is displaced vertically by about 10 cm to record the flux change $\Delta\Phi(z)$. Detection is performed with a 2nd order SQUID gradiometer. The water bag visible in this figure simulates the diamagnetic tissue.

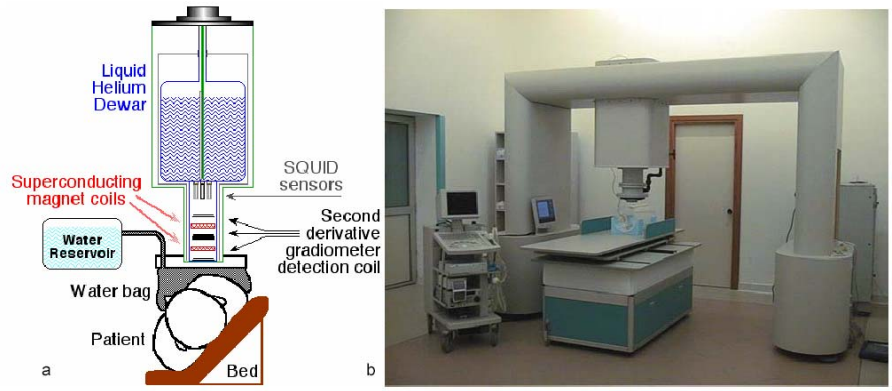

Fig. 3. Liver susceptometer: (a) Schematic diagram with main components [6] (reproduced with permission); (b) installed Ferritometer® system with an ultrasound scanner (to left of gantry) and a plastic calibration phantom (on the bed). Courtesy of Tristan Technologies.

Susceptometry is currently used to replace periodical liver biopsy when monitoring life-saving pharmacological therapy to reduce iron in the livers of patients suffering from ß-thalassemia and sickle cell disease. The liver of a normal subject contains 50 to 500 µg of iron per gram of this organ, while pathological iron overload may reach 5000 µg/g [6,36]. The detection sensitivity of a SQUID susceptometer is on the order of 10 µg/g, but environmental and physiological noise limits the system resolution to approximately 300 µg/g. While the numbers of iron overload patients are incomparably smaller than those of cardiac patients, the method is clinically accepted and rather well established, because of its demonstrated tremendous advantage to patients. As the number of installed systems is very low, patients are periodically travelling to diagnostic centers in Europe and in the US. Since its introduction in the 1980s [37], liver susceptometry helps thousands of patients every year. We are not aware of a manufacturer of commercial liver susceptometers in Europe. Tristan

Technologies of San Diego, CA, USA, is probably the only such company worldwide [38]. Their Ferritometer®, shown in Figure 11 (b) is based on that originally developed at Biomagnetic Technologies [39]. In Europe, significant contributions to perfecting the susceptometry and the present commercial system were made by Roland Fischer of the Eppendorf Hospital, University of Hamburg [36].

E. Low-Field Magnetic Resonance Imaging

The newest and currently most dynamically pursued biomagnetic method using SQUIDs as detectors is the magnetic resonance imaging (MRI) in very low, microtesla magnetic fields, already mentioned above in conjunction with MEG (Subsection II.A). However, microtesla MRI may well have a future independent of MEG, because of its potentially low cost and high imaging contrast between tissues. Even though the spatial resolution is perhaps a factor of two less than that of conventional 1.5 T MRI, one of the advantages of LFMRI is that it could be used to diagnose of all patients. At present, a not negligible fraction of the population having access to MRI cannot benefit from it. These patients cannot tolerate the confinement and/or noise or are simply too obese to fit into the patient space within the system's magnet. At microtesla fields, the MRI system can be essentially open. The 2007 status of the field and principles of LFMRI are presented in [28, 40].

The feasibility of low-field nuclear magnetic resonance (NMR) on room-temperature samples using a SQUID amplifier detector was first shown by Seton *et al*. at the University of Aberdeen, Scotland, in the context of the development of a low-field MRI scanner [41]. The authors used a tuned SQUID operating at about 425 kHz, the Larmor frequency in the magnetic field of 0.01 T. Their initial development work culminated in the demonstration of *in vivo* imaging of the human forearm [42]. The relatively low measuring field could be much less homogeneous than in conventional MRI, a major technical and cost advantage, and the SQUID improved the SNR compared to that of a room-temperature amplifier. Although this European work continued, the center of gravity shifted soon to Berkeley. The Clarke group moved to low microtesla fields thus further easing the field homogeneity requirement, while the acceptable SNR was assured by prepolarization in millitesla fields. The low (a few kHz) Larmor frequency made the use of an untuned SQUID amplifier advantageous. This work also culminated in human body imaging, together with the demonstration of high tissue contrasts, and the feasibility of prostate cancer detection. The latter is not possible with conventional MRI [28]. Brain imaging for MEG, and LFMRI for other applications have been then pursued at LANL [30] [3]. Further European work was then conducted by Burghoff *et al*. at PTB-Berlin, where nanotesla NMR and MRI measurements were first performed in their world-best MSR [43] and applied to studies of heteronuclear *J*-coupling and ^{1}H relaxometry. Finally, the possibility of NMR in the Earth's field using a high-T_c SQUID was reported by Qiu *et al*. of Jülich [44].

F. Concluding Remarks and Outlook

Of all applications of SQUIDs, biomagnetic systems, especially MEG, have been incorporating the highest number of implemented SQUID devices. However, the number of systems in the field is rather low (between 100 and 150 worldwide). In spite of the relatively

[3] For example, a multichannel LFMRI has been recently demonstrated in security application (liquid explosive detection), see ESNF paper ST114; NMR of UF6 for 235U Detection and Characterization was also demonstrated, see ESNF paper ST94.

long development period, biomagnetic applications have not yet found broad acceptance in diagnostic medicine, which would be commensurate with their potential. There are multiple reasons for this situation. Certainly, the relatively high system cost, the need for inflexible magnetically shielded rooms, and the use of cryogenic cooling are adverse, but not the most decisive reasons. Diagnostic MRI is more expensive, also requires some shielding, and generally utilizes liquid-helium-cooled magnets.

In our opinion, more decisive are two facts: (1) MEG and MCG offer only functional, but not anatomical imaging vastly preferred by medical practitioners, and (2) the conventional MRI, which also offers some functional imaging in addition to anatomic visualization, represents an enormously high investment by the major industry, with ensuing steady and fast progress in MRI diagnostics. Unavailability of industrial funding for statistically valid clinical trials is certainly the main cause of the lack of MCG acceptance. It is possible, but by no means certain, that integrating MEG and even MCG with low-field MRI could change that situation in the future. It is also possible that SQUID-based LFMRI of the human body and selected organs will be commonly used in cases where conventional MRI is impossible or impractical.

III. APPLICATIONS IN ELECTROMAGNEIC RADIATION AND PARTICLE DETECTION

A. Introduction

In astronomy, materials analysis, and also biology, SQUIDs are used mainly as amplifiers of signals generated by extremely sensitive superconducting detectors of electromagnetic radiation or particles. Perhaps the most representative of such detectors are transition-edge microbolometers (TES) used in the wide frequency range from microwave to X- and gamma-rays. These detectors are voltage-biased and deliver current response signal to be amplified by the SQUID ampere-meter.

Cryogenic temperatures, down to the 10 to 100 mK range, are most favorable for performance of sensitive detectors so cooling of the SQUID amplifier is not an issue. Readout of detectors is the most recent and still nascent application of SQUIDs, made possible by multiple demonstrations of superconducting detectors superiority over their semiconducting counterparts in terms of sensitivity, speed and energy resolution. This new application has been stimulated mostly by the needs of new, increasingly international astronomical projects and space missions calling for radio-telescopes and bolometer cameras with large arrays of detector pixels. The development of superconducting arrays for such projects started initially in the US, where major contributions to TES detectors, array SQUID amplifiers and multiplexers were made [40]. For larger arrays, the wiring complexity and related cooling power requirements make multiplexers (MUXs) necessary and unavoidable. The first large multiplexed arrays, with hundreds to over 1000 pixels were tested successfully, operate in the field and produce useful data. While these projects involve also European astronomers, the arrays have been developed in the US, at NIST, Boulder, and at UC Berkeley.

Boosted by scientific applications in astronomy, low temperature detectors are also in early stage of industrial applications. Various types of material analytical spectroscopy rely on the detectors' capability for energy-resolved single photon counting in the X- and gamma-ray bands. This application has been pioneered by NIST as well. However, also in Europe the first commercial spectrometer systems are now available [45]. Passive security

cameras for terahertz waves are another example of an application in a non-scientific environment [46].

The European work using SQUID readout is progressing with some time lag behind the US effort. The multiplexer development to date emphasized semiconductor circuits, but frequency-domain (FDM) and time-domain (TDM) MUXs involving SQUIDs are also being developed.

B. Amplifiers

The requirements for SQUID amplifiers as current sensors are readily achievable. However, in arrays the need for multiplexing intensifies the requirements, especially with regard to broadband signals and high scanning speeds. In current European work, series arrays of 10 or 16 SQUIDs are typically used as input stage amplifiers attaining high gain and low noise. Such amplifiers were mentioned in Part I, Section V.A; an example is described in ESNF paper ST2. In addition to high gain, the input array amplifiers must have: (i) a very wide bandwidth, on the order of at least 10 MHz, (ii) high dynamic range, and also (iii) very low noise temperature and low input impedance [40]. Furthermore, the amplifier noise should be lower than that of the detector itself. The required dynamic range, *i.e.*, the ratio of the bias voltage carrier amplitude and the detector noise, should be on the order of $\pm$ 10^6 $Hz^{-1/2}$. This requires negative feedback for sensor linearization.

Unfortunately, the standard SQUID flux-locked-loop does not offer the bandwidth required in some projects. Bandwidth is limited primarily by the delay in transmission line to room-temperature feedback electronics. Several approaches have been pursued recently to overcome this limitation. One, initiated by Kiviranta, consists of radical shortening of the delay line by using a low-noise cryogenic SiGe bipolar transistor as the second-stage amplifier of the signal from the SQUID array [47,48]. Another, pioneered by Drung *et al*., uses a large series array of low-inductance SQUIDs (up to 640 of these) as large-dynamic-range output stage providing the fast feedback signal [49]. De Korte *et al*. introduced the use of baseband feedback to decrease the required circuit bandwidth of the FDM MUX (10 MHz) to that of the signal (10 kHz) [50]. Neither of these approaches has been thus far implemented in practical arrays. Amplifiers in operating arrays with either TDM or FDM MUXs use room temperature feedback [51]. The only European array, which passed in-field tests and is now commissioned as a facility at the APEX telescope, also uses a room-temperature FLL [52]. This SABOCA camera, discussed below, doesn't impose special requirements due to the relatively narrow bandwidth of the astrophysical signal.

C. Multiplexers

The collection of signals from arrays of detectors to a common output channel, *i.e.*, the multiplexing, can be done serially (in the time domain) or in parallel (in the frequency domain). In time-domain multiplexing, each detector is read out by the first-stage SQUID amplifier. In a row of such amplifiers sequential bias switching selects one SQUID at a time, while the sum signal of a row is read out by a second-stage SQUID amplifier with an FLL. The switching rate is usually limited by thermal properties of detectors and switching itself is an additional source of noise. In the case of FDM, the sensors are ac voltage biased at different frequencies and read out as amplitude-modulated signals at the carrier frequency. Thus far, many European array designers appear to favor semiconductor FDM or TDM

combined with SQUID amplification. In one TDM case, a cryogenic SiGe ASIC[4] has been demonstrated to read out a small 2 x 4 pixel array [53]. However, one may doubt the practicality of scaling up cryogenic ASICs for large arrays, because of the cooling power limitation.

The only European array already tested in-field (SABOCA, see also next subsection) uses a 2-stage SQUID amplifier with a time-domain multiplexer scheme, shown in Figure 4 [52]. The first-stage is a row of 10 SQUIDs, fabricated on a common chip and kept at T=300mK. Each SQUID has a gradiometric current sensor layout; the typical noise is around 5 $\mu\Phi_0 Hz^{-1/2}$. The output sum is fed into the input coil of a second-stage SQUID (actually a SQUIF amplifier) at the next cooling stage (between 1.5K and 3K). All control electronics, *i.e*., the switching of the bias currents of the SQUID array and the FLL for the amplifier SQUID are at room temperature. The output signal is digitized (24bit), and a FPGA controller processes the digitized data and reallocates (demultiplexes) them. The switching between the SQUIDs in the array is done at 2kHz rate, because the high-precision data acquisition cannot follow faster jumps in the signal. Even at 2kHz switching, half of the cycle is the settling time. The multiplexing itself can be much faster, up to 100kHz. The total noise in the MUX mode is about $20\mu\Phi_0 Hz^{-1/2}$. The current noise of the bolometer itself, converted to flux noise, is typically $100\mu\Phi_0 Hz^{-1/2}$, so the MUX does not dominate the signal.

A successful proof-of-principle test of a simplified TDMUX using superconducting-to-normal SQUID switches was lately reported [54]. Its topology ensures that there is no noise contribution from "off" channels, which are all short-circuited by switches in superconducting state. A conceptual design of a superconducting FDMUX entirely based on SQUIDs was also reported [55,56], but we are not aware of any test data.

Perhaps the most promising for the future of very large detector arrays is the microwave frequency-domain multiplexer recently demonstrated at NIST [57]. Superconducting high-quality-factor Q coplanar resonators with different frequencies couple to a common transmission line, while each resonator couples to a different dispersive (thus dissipationless) rf SQUID. A flux-ramp modulation scheme linearizes the response of each pixel without a separate feedback signal. In the prototype demonstrated, 32 resonators were nearly evenly spaced in the frequency range between approximately 4 and 6 GHz and had intrinsic Q between 20,000 and 40,000 (the coupled Q was an order of magnitude lower). The rf SQUID measured flux noise was only 0.17 $\mu\Phi_0/Hz^{1/2}$; the equivalent current noise was 100 $pA/Hz^{1/2}$ comparable to the noise of a standard low-noise TES design.

[4] Application-specific Integrated Circuit

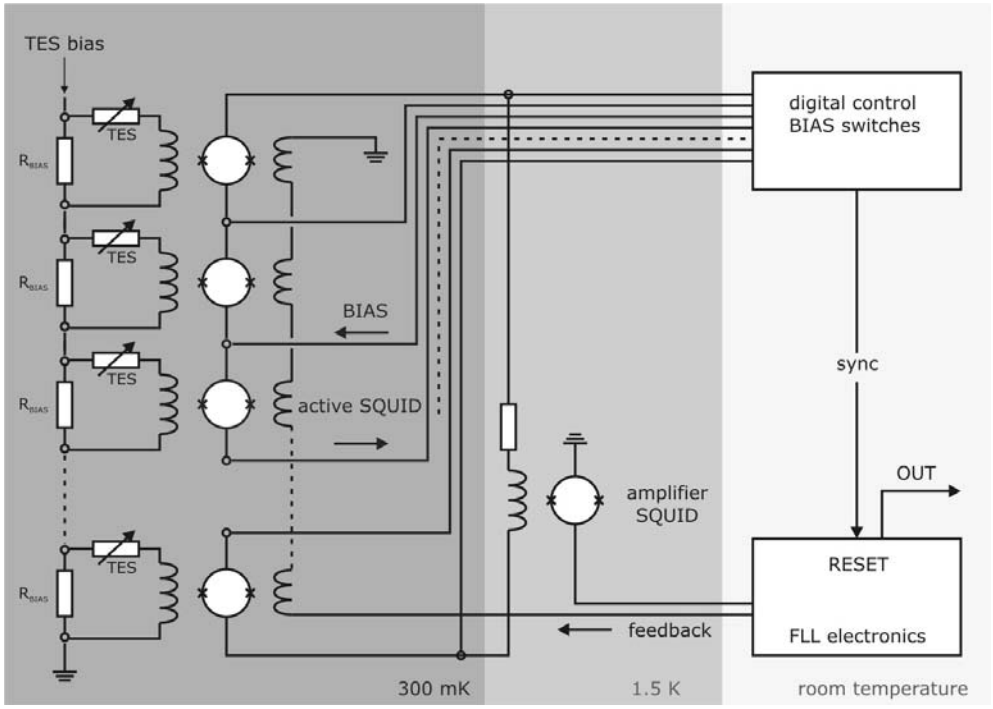

Fig. 4. Simplified schematic of the time-domain MUX of SABOCA-2 and LABOCA-2 arrays. Courtesy of T. May, IPHT.

D. Astrophysical Projects and Space Missions, Outlook

Thus far, three relatively large cameras for stationary radio-telescopes are the most successful astrophysical projects involving multiplexed microbolometer arrays with SQUID circuitry. The most ambitious, SCUBA-2, is currently being installed at the Maxwell telescope in Hawaii. This project, a submillimeter wavelength camera with more than 10,000 pixels in its final configuration read out by TDM, will substantially increase data acquisition speed in large-scale cosmological surveys. Topics of interest here are elliptical galaxy formation, the star formation history of the Universe and of our own galaxy [58]. The other two, the APEX-SZ 320-pixel camera for the APEX Telescope (12 m diameter) on the Atacama plateau in Chile, and the 1000-pixel camera of the 10 m diameter South Pole Telescope (SPT) use arrays with FDM, operate at 95, 150 and 220 GHz and are used for the study of galaxy clusters using the Sunayev-Zel'dovich effect (SZE) [59]. The first ever galaxy cluster discoveries via this effect (using APEX-ST) had already been reported [60]. Other array projects are in progress on a similar scale; see [61] for an example.

The first successfully tested European camera is the 40-pixel SABOCA, a technology test at 350 μm wavelength preceding larger cameras intended for large-scale mapping of skies at millimeter and submillimeter wavelengths [52]. It is a project of Max Planck Institute for Radio-astronomy, (Bonn, Germany) in collaboration with IPHT-Jena. Their work in progress includes LABOCA-2, a 300-pixel camera for operation at 870 μm wavelengths. A 1000-pixel camera (350 or 870 μm) is planned.

Bolometer arrays for space missions are at the stage of advance exploratory studies and of low-scale demonstrators to enable the assessment and the choice of most appropriate and sufficiently mature technology. Current European work involving SQUID readout of arrays is largely motivated by future space missions. Among them is the International X-ray Observatory, IXO. One of the core instruments on IXO should be an imaging spectrometer.

The current EURECA project aims at demonstrating flight readiness for such future X-ray astronomy missions [50]. The prototype instrument will consist of a 5 × 5 pixel array of TES-based micro-calorimeters to be readout by frequency-domain-multiplexed SQUID amplifier channels. The FDMUX with digital baseband feedback will be in semiconductor technology. Currently, VTT and PTB are developing SQUID amplifiers for this FDM MUX to optimize the dynamic range, low input inductance and cable driving capability.

Larger microbolometer arrays are under development for the SAFARI instrument to be installed on the Japanese SPICA mission. Large arrays (up to 64 x 64 pixels) of very sensitive bolometers (noise equivalent power, NEP $\approx 2\ 10^{-19}$ W/$\sqrt{}$Hz) are to be read-out by FDM MUXs. [62]. The hardware development is under way using SQUIDs developed at PTB.

Other ambitious space missions are contemplated. An example is the proposed B-Pol mission aiming at mapping the polarization of the cosmic microwave background radiation using an array of about 400 TD multiplexed TES [63]. A similar, but ground-based, telescope project CLOVER was the recently cancelled due to curtailing of funding, but a TES study for focal plane arrays was reported [64].

Large microbolometer arrays are being developed for other research purposes as well. In Europe, a prominent example is the proposed exact measurement of neutrino mass via β decay in the MARE project [65]. Initially, a 300 pixel Ir-Au microbolometer array with FDM is under study, eventually a very large array of 50,000 pixels is hoped for [55].

Cryogenic detectors with SQUID readout also hold promise in sensitive detection of biological molecules. For example, in a study of matrix-assisted laser desorption/ionization time-of-flight mass spectroscopy, use of a cryogenic Ir-Au bolometer resulted in lowering of detection threshold for insulin by several orders of magnitude [66].

The whole field of SQUID applications in detector arrays is still in the initial stages of development and is experiencing a high rate of progress. This subsection has been intended to provide only an incomplete snapshot of the status in early 2009.

IV. NONDESTRUCTIVE EVALUATION OF MATERIALS

A. Introduction

Electromagnetic methods of non-destructive evaluation (NDE) of conducting materials (usually metals, but also semiconductors and laminates such as carbon fiber reinforced plastic (CFRP), typically focus on one of three approaches for the detection of flaws due to corrosion or other damage to the subject under investigation. In the first, an electric current (dc or ac) is injected or induced into the specimen, and the distortion of the associated magnetic field as it flows around the flaws is detected by an appropriate sensor. In the second, a pulsed magnetic field is applied to the specimen, inducing a current whose subsequent decay is measured and spectroscopically analyzed to produce information on the depth distribution of resistivity and thus flaw location. In the last, which is largely reserved for materials which are at least weakly magnetically susceptible, and more usually ferromagnetic, the specimen is polarized by an applied magnetic field: a flaw then distorts the spatial field distribution in a way that can be analyzed to spatially locate it. As we shall see, spatial resolutions, which at first were limited to a minimum of a few mm, have now been reduced to a few tens of μm and can be expected to fall further in future.

Traditionally, NDE engineers have used Faraday induction coils as their sensors, though other probes such as Hall and giant magnetoresistance (GMR) devices have also been used. SQUIDS were introduced in the mid-1980's by Donaldson *et al* [67] and Weinstock and

Nisenoff [68], and their use has been steadily extended since then, particularly in Europe, which has been a world-leader in many ways, especially in developing high-T_c SQUIDS and techniques for NDE. Particular leadership has been shown by the groups at Research Center Jülich (FZJ) [69] and at the Universities of Strathclyde [70], Giessen [71], Naples [72] and Jena [73]. However, there have also been significant contributions from groups in Japan, Korea and India.

It is important to realize at the outset that the use of SQUIDs is not normally associated with exploitation of their extreme sensitivity (femtotesla level) required in biomagnetism. Rather, the properties utilized include their vector and field differencing capabilities (*e.g.*, of a gradiometer- see Part I) and also their ability to resolve a tiny change of field in the presence of a large background one. Indeed, a significant European contributions has been to the design of current excitation and gradiometer detection structures suitable for scanning NDE, especially in unshielded environments [74], and above curved structures such as aircraft wings [75].

The final most important property of SQUIDs for NDE is their sensitivity down to very low frequencies, far below the limits of Faraday coils (~ 300Hz): in cases where electromagnetic skin depth is a consideration, this allows probing for flaws at depths considerably greater than those possible with traditional eddy current methods.

We now turn to a more detailed discussion of each of these approaches. Note that the description of NDE 'material' can extend to the detecting the conductance anomalies caused by minerals in geological and archaeological substrates: the use of SQUIDs in geophysics is covered in the next section.

B. Direct Current Polarization

The earliest NDE use by Donaldson *et al.* [67] involved the polarization of ferromagnetic steel plates by a dc magnetic field of about 0.02T, which, produced as it was by a superconducting coil in the persistent mode, was perfectly constant in time: it therefore generated no signal in a pickup gradiometer connected to a SQUID. However, when a plate with a flaw (crack, or dislocation field produced by mechanical fatiguing) was pushed beneath the gradiometer, the permeability variation (typically 50%) associated with the defect produced a distortion in the polarizing field, and thus a change in the flux coupled to the SQUID. Surface breaking flaws with a cross-section as small as 0.1mm×0.1mm could be detected. It was shown that when a plate was cracked along part of its length by repeated flexure, the permeability reduction due to work hardening extended considerably beyond each end of the actual crack.

A very significant extension of this basic 'flux leakage' technique was its application to the detection of water-induced ruptures in the prestressed steel tendons (rebars) in beams forming parts of civil engineering structures such as bridges [76]. In another application, Tavrin was able to detect the presence of metallic inclusions in the turbine blades intended for use in high speed gas turbine aircraft jet engines [77]. Undetected, these could lead to catastrophic fracture failure in service. This method was licensed and used by a jet engine manufacturer.

C. Current distortion

The effect of a flaw on an induced, or less commonly injected, current is to divert it, and to produce a field external to the specimen which is typically dipolar This can be detected by a SQUID gradiometer, which is usually configured as a double-D. Although the first

demonstration of this method used an injected direct current, it is now more usual to induce an alternating test current using an external excitation field, and to detect the distortion field due to the flaw synchronously with the excitation.. The method can 'see' into the specimen up to the skin depth ($\delta = \pi\mu\sigma f)^{-½}$ where μ, and σ are respectively the permeability and conductivity of the specimen, and f the frequency of the excitation: δ is typically 2.6 mm for a 1kHz excitation in aluminum. In the past decade, the Julich group was world leader in developing such eddy current techniques [78]. One of the first practical uses of eddy current testing was the detection of partially developed cracks in the wheel hubs (see Figure 5 for their construction) of Lufthansa planes [79]. Figure 6 shows the detected signal versus the wheel rotation angle for various artificial flaw depths. It proved possible to detect cracks down to a mere 10% wall penetration with a high-T_c SQUID rigidly mounted close to the rotating wheel. Alternatively, the SQUID could be spatially scanned above a fixed aircraft element such as a row or rivets in an aircraft wing or body [80]. By operating at frequencies as low as 22Hz, cracks as deep as the second aluminum layer (31 to 46 mm below the external body surface) have been detected in an Airbus 300.

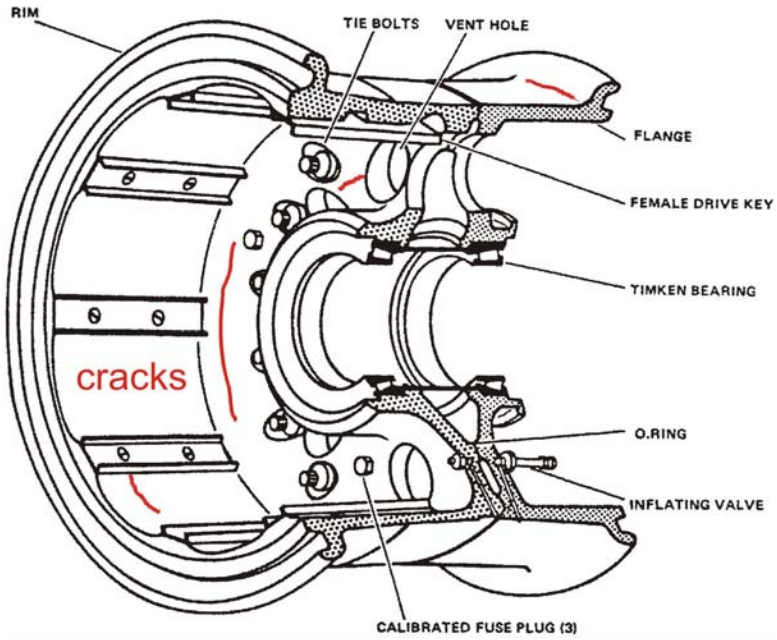

Fig. 5. Structure of an aircraft wheel hub in which there are a number of partly through cracks. Courtesy of J. Krause, FZJ.

Mück has developed eddy current techniques using a low-T_c SQUID to detect very small inclusions of tantalum impurity in niobium sheets intended for use in rf superconducting cavity resonators for particle accelerators [81]. Such inclusions can have deleterious effects on the very high Q factors required. Because the two metals have very similar conductivities the current distortions produced by the inclusion are very slight, but they can be detected by the SQUID system. Particle sizes down to 10μm have been detected.

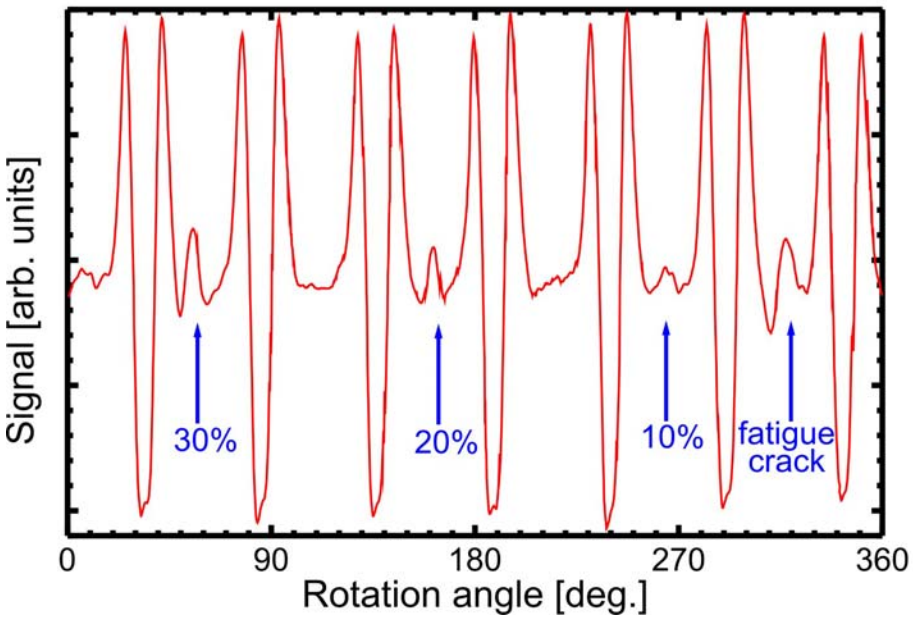

Fig. 6. SQUID signal as the wheel hub of Figure 2 is rotated beneath a fixed HTC SQUID cooled by a portable cryocooler. Courtesy of J. Krause, FZJ.

D. Layered Materials

The technique has been extended to the important modern aircraft material carbon fiber reinforced plastic (CFRP), which is very susceptible to delamination of its layers due to small body impact, and, moreover tends to exhibit damage on the far side of a CFRP plate which has been impacted. Such material presents two types of problem. First, because it is layered, it is very anisotropic. Second, because it has very low conductivity (in-plane it is some 10^4 times smaller than in aluminum), NDE signals tend to be much smaller than in the case of metals and may be buried in noise. The Naples group has made significant progress here [82]. However, perhaps the work most worthy of further development has been that of Graham *et al* [83], who developed neural network methods for recognizing NDE spatial patterns within this noise, and showed a capability of locating flaws within a horizontal resolution of a few mm. Because skin depths tend to be large enough to 'see' through to the far side of a typical plate, the method can detect a flaw that might otherwise be inaccessible, being on the inside of a wing structure. A typical 'neural net' result is shown in Figure 7.

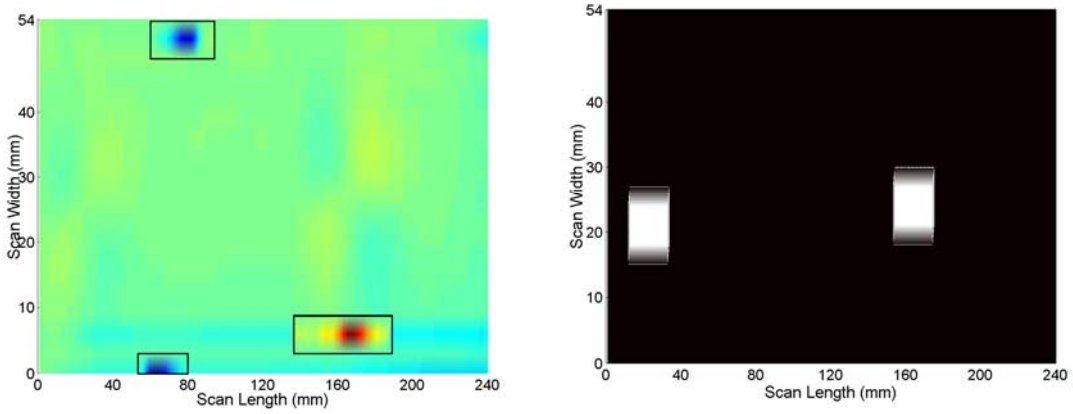

Fig. 7. Left: data from a scan of a CFRP plate in which noise has caused the SQUID to lose lock several times resulting in spikes in the data which obscure the signal arising from two defects. Right: The results of applying a neural network system to this data. Both defects are detected and their centers identified [83]. Courtesy J. Krause, FZJ.

E. Scanning SQUID Microscopy

Recently, NDE methods known as Scanning SQUID Microscopy (SSM), which achieve much higher spatial definition than those discussed earlier, have been developed[5]. Typical characteristics of SQUID microscopes are tiny magnetic field detectors (coils or others) with lateral dimensions on the order of a few tens of microns or less, and a very small separation (stand-off) between the pick-up and the surface or object of interest, which can be magnetic particles, magnetized surfaces, flux vortices in superconductors, biomagnetic objects, and current flows. The objects analyzed can be at cryogenic or ambient temperature and the SQUIDs either low- or high-T_c. The probe is usually at cryogenic temperature, but occasionally it can be at room temperature. It is *x-y* scanned relative to the object under study so that the microscope output will be a magnetic map, whose data can be processed to extract the underlying information which is sought. Detailed information can be obtained from [84] and a number of more recent review articles, such as that by Mück [85], and we here discuss SQUID microscope methods only briefly.

Reference [84] distinguishes four types of SSM; we discuss three. In the first, both pickup and sample are cold, and the SQUID(s) fabricated on a chip, in a way which brings both into physical contact. In the second, the SQUID and pick-up coil are cooled, but the sample is at room temperature. They must be as close as possible and so windows separating their two regions of thickness down to 20 μm and comparable lateral dimensions have been produced. Resolutions of 20 μm can be achieved, and in a commercial form (NEOCERA SSM), this system has been applied to mapping current flows in computer circuits and detecting faults [86]. In practice [87], the effective resolution can be much better. In the third system, the sample object is at room temperature, and its flux collected by a sharp high-permeability magnetic needle penetrating the cryogenic envelope, and brought to close proximity (micrometer distance) of the sample [88]. The fields from the sample polarize the needle, which becomes a flux focuser coupling them to the SQUID.

[5] SSM is a special case of scanning magnetic microscopy, SMM.

The most prominent application of SSM is probably testing of computer circuits [86]. European uses of SSM include magnetic dipole imaging in ferromagnetic samples [89], and study of magnetic relaxation in nanoparticles for magnetic storage media [90].

F. Transient Electromagnetics (TEM) Technique in Metals

An extension of the eddy current method is the use of TEM techniques in metals, rather than geophysical structures, which are discussed in Section V. A short electromagnetic excitation pulse induces eddy currents whose frequency components cover a wide range of frequencies, and thus a range of penetration depths. If the eddy current signal is sorted into a number of time epochs, the later times will correspond to lower frequencies and thus to greater depths. With a single pulse it therefore becomes possible to do a complete depth profile of the conductivity of the specimen, and thus to determine how far below the surface any flaw is located [91].

G. NDE of Semiconductors

An original approach to the study of spatial variations of doping in semiconductors was introduced by Beyer *et al* of PTB [92]. A 675 nm wavelength laser illuminates the underside of a wafer of order 0.5mm thickness with a spot of 20μm diameter, and excites photocarriers which interact with the internal electric field associated with any spatial change in dopant concentration. The resulting electric currents produce magnetic fields proportional to the local dopant concentration gradient which are detected by a flux-locked SQUID system mounted on axis with the laser beam. The beam and SQUID are scanned in a conventional *x-y* mode, resulting in a map of dopant concentration. For fluctuations in dopant level of a few percent about the nominal value, lateral resolutions of a few tens of μm were obtained in nitrogen doped silicon.

H. Future Prospects

Though significant progress has been made in many aspects of SQUID NDE, its general acceptance has many hurdles yet to overcome. Perhaps the most significant is that the methods of conventional NDE are highly various, and only a few might be suitable for replacement by SQUID technologies (*e.g.*, in the aircraft industry). The market for such SQUID instrumentation is small, and acquisition costs are in the few tens of thousand dollars per unit. The challenge is to try to produce SQUID base units which are low cost, portable, and capable of use in any orientation. In this respect work on a system readied for use by a cryocooler which is then disconnected and removed, leaving a compact arrangement kept cold by a 'cryobattery' which will keep the SQUID within its operating temperature range for many hours, showed promise [93]. It requires a number of further cycles of practical development, however, before it could come into wide use.

GEOMAGNETIC AND RELATED APPLICATIONS

A. History and Method

The use of SQUIDs for geomagnetic exploration, specifically prospecting for oil and minerals, has a rather long history. Indirectly, initial research into the use of SQUIDs in magnetotellurics for oil exploration, performed by John Clarke's group at Berkeley at the end of 1970s and beginning of 1980s, significantly advanced the prospecting methodology then in use, even without any SQUID involvement, by introducing remote referencing [94,95].

Geomagnetic exploration using SQUIDs shares many similarities with magnetic anomaly detection (MAD) for military purposes, which had not been recently pursued in Europe, and also it had not lead there to published results of major significance. What had been published earlier on military MAD can be found in [96]. Therefore, we limit our attention only to the very successful recent development work at IPHT, and mention similar developments by CSIRO in Australia. The CSIRO group pioneered the use of mobile SQUIDs, essentially high-T_c, for prospecting of minerals [97,98]. Equipment developed by both groups in the late 1990s has been gradually perfected, and in the current decade introduced into the field use by commercial companies performing exploration for minerals. It soon became a real success story[6]. Both groups concentrated on the same exploration methods: transient electromagnetics (TEM), which is suitable for ground-based and airborne prospection (surveying) for conductive mineral ores, and geomagnetic prospection for magnetic ore bodies.

B. Transient Electromagnetics: Ground-based

The principle of TEM is presented in [96]. Here it suffices to say that it is an active method consisting of (a) emitting long sequences of strong magnetic "primary" pulse signals from a suitable transmitter feeding a suitable antenna, and (b) recording the "secondary" response of magnetic field signals due to currents induced by conductive ores in the ground. From the decay time of this response one can infer the depth of conductive signal sources, as already explained in Section IV with application to NDE of metals, which preceded any TEM use in geophysical exploration. A rough estimation of depth can be obtained from the skin depth model. The TEM method requires intense signal averaging to attain a sufficient SNR. The pulse transmitter and room-temperature data acquisition electronics have been standard commercial exploration equipment for some decades.

In the ground-based TEM, a large loop transmitter antenna, 100 to 500 m by side, is positioned on the ground, while the sensing device, a large Faraday induction coil with room-temperature amplifier or a SQUID sensor, is moved along a suitable surveying path within or near that antenna loop, in the, so called, fixed loop arrangement. The superiority of a SQUID magnetometer sensor over the conventional Faraday induction pickup coil resides in the direct measurement of secondary signal field rather than field derivative dB/dt, which decays faster. In the example shown in Figure 8, SQUID could follow up the signal decay with acceptable SNR up to a second, while for a very large Faraday pickup coil (size of transmitter antenna) noise dominated the signal already after 10 milliseconds. This is shown in Figure 8 for two conventional amplifier gains, 10 and 1000. The factor of 100 longer useful measuring time translates into a factor of ten greater depth detection.

[6] In 2007 IPHT was awarded first prize by the renowned Mining Journal "for groundbreaking research in geomagnetic surveying systems".

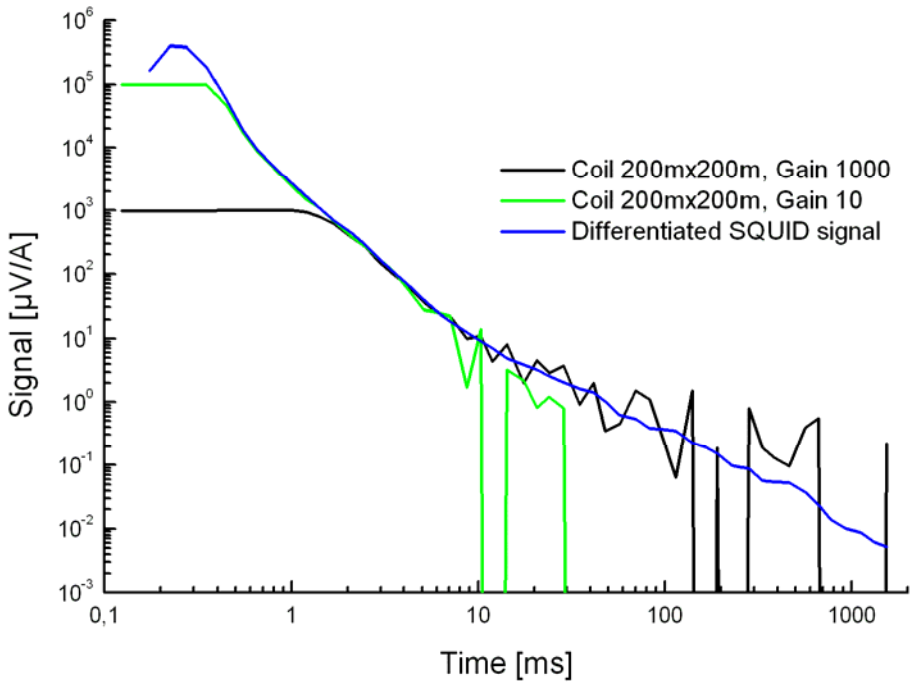

Fig. 8. Signal decay curve for standard Faraday coil at two room-temperature amplifier gains, in comparison with the signal recorded by a high-T_c SQUID. For easy comparison, the SQUID signal was differentiated. The SQUID effective gain isn't given. Courtesy of R. Stolz, IPHT.

This superiority was convincingly demonstrated in the field using high-T_c magnetometers first developed at CSIRO [99,100]. Their portable system LANDTEM was licensed to industry. The portable high-T_c system prototype developed at IPHT is concisely described in [101,102].

Many details of current IPHT ground-based TEM systems are proprietary. Some ground-based TEM exploration systems build by SUPRACON [103], developed with and licensed by IPHT, are used in mineral exploration in Africa and Canada. The demand for such systems is rather low, so one small company can satisfy it. According to CSIRO, the demand for their high-T_c ground-based TEM systems licensed to an exploration company is rather high [104].

C. Airborne TEM Surveying

Airborne surveying is the most practical and fastest method for detection and preliminary localization of ore deposits. In the case of the TEM method, the transmitter coil and the sensing antenna are installed in the airborne platform. This can be either an airplane or a helicopter. There is a variety of different transmitter geometries:

(i) A coil around the airplane and a receiver inside a "tow bird", *i.e.*, a separate container towed by the aircraft (commercial Spectrem 2000 and Fugro systems [105]). The receiver can be suspended to reduce rotation effects, as is the case of the CSIRO's experimental high-T_c SQUID system.

(ii) A tow bird with both a transmitter coil and a fixed mounted receiver (the commercial VTEM system [106]).

(iii) A receiver placed in a second tow bird, above that with transmission coil.

The main argument for using a SQUID rather than a Faraday coil detector is the same as for ground-based TEM: the possibility of detecting ore deposits at greater depths and with better sensitivity and spatial resolution. Considerable work in this direction was performed mainly at CSIRO [107], but more development work is required.

D. Airborne Geomagnetic Exploration Systems

Airborne geomagnetic exploration is entirely *passive* and consists of detecting magnetic anomalies caused by magnetic remanence of mineral ores. The surveying equipment is installed in a fixed "sting" rigidly mounted in the tail of the airplane or in a tow bird. Both alternatives aim at minimizing exposure to the strong electromagnetic noise of the aircraft. The aircraft flies along a predetermined straight-line raster path at an altitude low enough to maximize sensitivity of magnetic anomaly detection while the instrument calibration occurs in high-altitude uniform Earth's field.

It is most desirable in surveying to measure the full tensor of the magnetic field and derive information not accessible from measurements of the total field or of vector field component(s). The principles of tensor gradiometry are presented in [96]. In airborne surveying, at least five independent gradients need to be measured. Tensor gradiometry enhances the definition of structural features, permits continuous mapping of the magnetization vector in source rocks, and of magnetic susceptibility distribution, *etc*., also by minimizing effects of the vectorial sensor misorientation [108]. More detailed and quantitatively interpretable geological maps result.

Operation from a mobile platform is the most demanding of all: the output should be invariant when moved and rotated in uniform Earth's field. This requires the highest possible CMRR of gradiometers. The well-balanced planar low-T_c gradiometers developed by IPHT have intrinsic CMRRs on the order of 10^5, but with compensation by correction signals from a less sensitive reference triple magnetometer (measuring the three components of $\boldsymbol{B}$) this value is improved by better than one order of magnitude. An early version of such gradiometers developed at IPHT, and briefly described in Part I, was published [109]; the design has been significantly improved since. The gradiometer base is 40 mm. An alternative system for in-motion cancellation of the three components of the Earth's field by active shielding via tri-axial Helmholtz coils for "global feedback", was proposed and proof-of-principle demonstrated with a possible application to military MAD [110]. It could significantly reduce the requirements for dynamic range and slew rate in tensor gradiometry. However, this hardware-intensive approach has not been followed in airborne surveying.

IPHT developed what is probably the world's most advanced geophysical SQUID system, the first ever for airborne full magnetic tensor measurements of magnetic field and field gradient components to localize and quantify magnetic targets [111]. Six balanced gradiometers and 3 magnetometers collect data in a bandwidth from dc to 500 Hz. Figure 9 shows the in-flight-recorded noise spectrum of a software-compensated gradiometer, compared with that of a bare gradiometer and spectra of the three magnetometers. The whole battery-operated unit has low power consumption (15 W) and is mounted in a LHe cryostat. When operated from a helicopter, additional ballast brings the total weight of the towed system to about 100 kg. The system is marketed by SUPRACON under the trade name "JESSY STAR". High spatial resolution is provided by a differential GPS system using the satellite-based augmentation system (SBAS) and an inertial unit (INU), which are synchronized with the magnetic gradient data. The INU data is used for additional motion compensation. The data acquisition system incorporates a small-sized 21 channel 24 bit and

12 channel 12 bit analogue digital converter units. In straight and level flight, CMRR of 10^6 can be maintained. Most details of the equipment are proprietary.

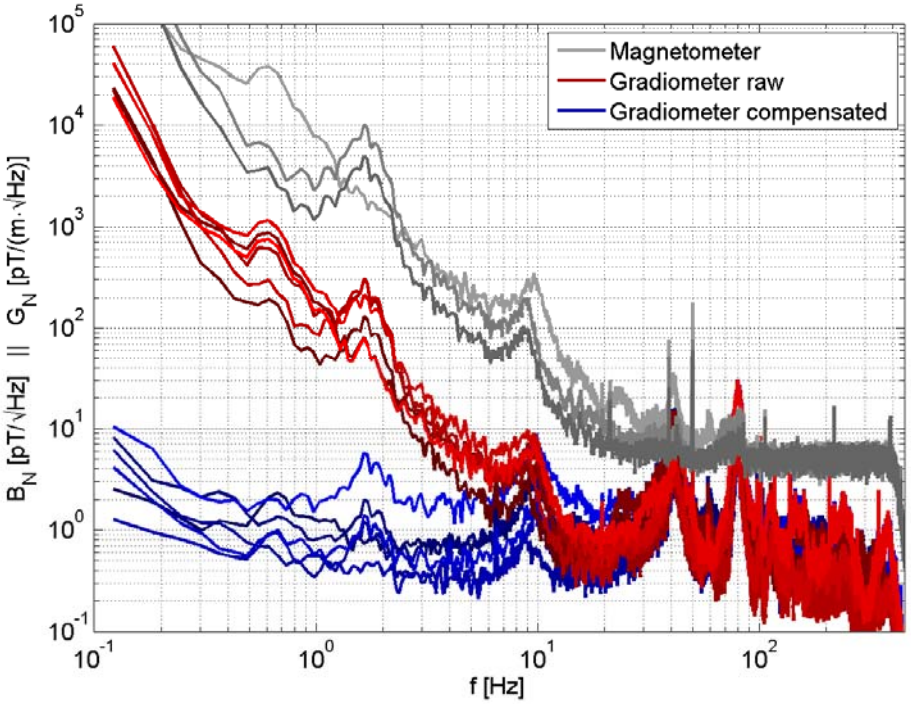

Fig. 9. In-flight-recorded noise spectra of the JESSY STAR system (recent performance): comparison of compensated gradiometer performance with that of bare gradiometers and of three system magnetometers. Courtesy of R. Stolz, IPHT.

E. Other Geomagnetic Applications

Magnetic surveying (prospection) is also used in archeology and sometime termed archeometry. The main motivation is to detect and image buried man-made objects and structures prior to or instead of excavation. Until recently, absolute cesium magnetometers have been used to detect magnetic anomalies. The introduction of high CMRR SQUID gradiometers results in significant improvement in sensitivity and surveying speed. The system introduced by IPHT is the precursor of their ground-based TEM apparatus, but the MAD is entirely passive and uses gradiometers [112]. Position referencing is also assured by GPS. The car-pulled cart, on which the equipment is mounted, is constructed entirely from nonmagnetic glass-fiber-reinforced plastic (GRP). The GRP dewar contains 2 liters of LHe permitting 2 days of operation between refills. The system capabilities were demonstrated by prospecting archeologically interesting areas in Peru.

Most recently, Waysand *et al*. have shown that a SQUID magnetometer located at a very deep and magnetically quiet subterraneous location is capable of detecting ultra-low-frequency oscillatory signals of collective charged particle displacements in ionosphere excited by acoustic waves from earthquakes many thousand kilometers away [113]. The authors expect their instrument to become a powerful tool for ionosphere studies.

Among the most speculative proposed applications of SQUIDs has been their use for the prediction of earthquakes and volcano eruptions. In the second half of XX century it was proposed that such large-scale seismic events have electromagnetic precursors possibly usable

as early warnings. Among ultra-low-frequency (Ulf) magnetic field measurements of what was presented as magnetic precursors some notoriety acquired those of Fraser-Smith *et al*. (Stanford University), who believed to have correlated the Ulf precursor signals with the rather strong Loma Prieta (California, USA) earthquake [114]. These measurements were made with induction coils, but it was only natural to propose that more sensitive SQUIDs will be usable for such purpose. Especially in Japan, some effort was expended towards the use high-T_c SQUIDs for such purpose [115]. It is very difficult to correlate Ulf magnetic measurements with seismic events by eliminating all other artificial and natural signal sources and statistically correlating beyond random chance. We believe no convincing proof of such a correlation has been presented to date.

F. Future Prospects

Geophysical and archeological prospecting using SQUID is gaining a growing commercial acceptance, in spite of the use of LHe cooling, largely because of the full gradient tensor capability, which the existing high-T_c systems don't have, and the superior noise performance at very low frequencies. However, the convenience and lower cost of using LN_2 cooling motivate continuing efforts to develop competitive full gradient tensor high-T_c systems. Of these, probably the most ambitious is CSIRO's project GETMAG, which involves gradiometers rotating about three separate axes [116,117]. The proof-of-principle was successfully demonstrated in the field, over a known magnetite deposit in Australia. However, the progress has been rather slow and a practical system has not been announced to date. We can only hope that the remaining difficulties will be finally overcome.

Looking into the future, one can also expect that the acceptance of SQUID surveying equipment by the mineral ore exploration companies will eventually lead to the exploitation of the performance advantages in hydrocarbon (oil) exploration, involving borehole sensor apparatus.

V. STANDARDS AND METROLOGY

A. Introduction

A very early application of the Josephson effect was, of course, to establishing standards of voltage, using the Josephson frequency relation. Two leading European groups in the field were PTB in Germany and NPL in the UK, fulfilling their mission as National Standards Laboratories. Indeed, PTB (together with NIST) is responsible for manufacturing the commercially available multi-junction chip that delivers up to 10V, for use as secondary standards in calibration laboratories. It is therefore no surprise that, when SQUIDS became available, these and other European laboratories looked for opportunity to apply them, in their turn, to standards and metrology, and we now turn to some of these. Further detail on some of these topics is available in [118]; see also RN9 of ESNF.

We begin with applications of SQUIDS to noise thermometry: recent work in Europe has focused first on improved measurement of Johnson noise in resistors, and secondly on a novel process (Quantum Roulette), whereby the distribution of thermally excited flux states in a SQUID ring is measured and in turn the absolute temperature deduced.

Thereafter we discuss the two types of Cryogenic Current Comparator, on whose development much recent progress has been made in Europe, and make mention of their applications to precision resistance ratio determination, to ultra-low current measurements,

including those delivered by SET devices, as well as to resistance measurements at high currents.

Finally we look at the SQUID-based SQUIF (Superconducting Quantum Interference Filter) a relatively recent introduction, which has a number of possibilities for systems applications as devices such as mixers, but very significantly, may make possible the measurement of precisely zero magnetic field, and in turn the ability to measure the absolute magnitude of a field, something not previously possible with SQUIDs.

We do not cover work towards metrological applications of SQUID-based qubits, because the qubit and quantum computing research involving SQUIDs are to be the subjects of a future issue of ESNF.

B. Low-temperature thermometry

The sensitivity of SQUIDs can be effectively used to improve existing techniques for the measurements of low temperatures and to create novel types of thermometers. Whereas usage of the former SQUID based thermometers was restricted to metrology labs, state-of-the-art SQUID technology enables novel user friendly thermometers for measurements down to the millikelvin and in the near future to the sub-millikelvin range.

Noise thermometry involving SQUIDS by measuring of the spectrum of Johnson noise developed in resistors is long established, but is as yet too sophisticated a technique to leave the realm of standards laboratories. In pursuit of this goal, PTB has developed thin-film resistive SQUIDs which show promise for use at temperatures down to 100 mK [119]. These chip based thermometers have not become of practical importance yet. For lower temperatures (down to 10mK), in collaboration with the Heidelberg group, PTB has developed a new magnetic field fluctuation thermometer, in which the SQUID measures the fluctuations in the field above the surface of a conductor, as produced by the Johnson noise currents within it. The device is rugged, fast, and is already commercially available [120]. In many cases it can replace the ^{60}Co nuclear orientation thermometer which is not accepted everywhere, because it contains radioactive material.

Instead of measuring the magnetic field fluctuations above the surface of the conductor one can measure the current fluctuations in a conductor directly with SQUID readout. This technique called current sensing noise thermometry has been intensively investigated by Lusher *et al*. from the low-temperature group of Royal Holloway University of London [121]. Integrated versions of a current sensing thermometer with a thin-film Pd resistor and read-out SQUID on a single 2 x 3 mm^2 chip have been realized at PTB allowing very fast measurements with low statistical uncertainty. Below 100 mK thermal decoupling of the electron system of the resistor causes increasing uncertainty of the thermometer [122].

An imaginative novel approach to absolute thermometry (Quantum Roulette Noise Thermometer) was recently attempted by Gallop *et al*. It used the multiple flux (and thus energy) states which can exist in a superconducting ring, interrupted by a weak link which can be used as a switch. A SQUID, coupled to the ring, reads out its flux state after each opening and closing of the switch, induced by a an applied magnetic field pulse. This allows a histogram of states to be built up, whose width determines the probability distribution of the occupation of these flux states at the temperature of operation, and can thus be used, in principle, as an absolute thermometer [123] as shown in Figure 10, which displays the spectrum of energy states at each of four different temperatures.

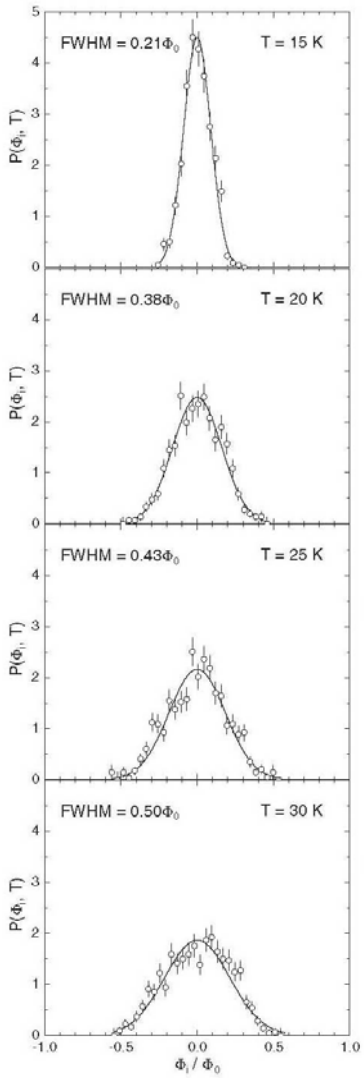

Fig. 10. Spectra of energy states at four different temperatures. Courtesy of J. Gallop, NPL.

It was originally intended that the experimental realization of this scheme would involve high-T_c rings and SQUIDs, and allow temperatures up to 70K or more to be determined. Proof-of-principle was demonstrated, but unfortunately the temperature variation of the proportion of *s*- and *d*-pairing in the high-T_c materials led to unacceptable inaccuracies above 40 K [124]. Prospects for the project became limited to low-T_c materials and to temperatures below 1K, but though there was a good scientific case for exploring this regime, there was little funding interest, and to date no experimental work has been done.

C. Cryogenic Current Comparator (CCC)

Although it was invented at CSIRO in 1972, the CCC had its most significant early developments at PTB [125] and NPL. Its principle is very simple and is illustrated in Figure 11, though the details of its highly accurate implementation are complex. Consider two wires, carrying currents I_1 and I_2 respectively, both passing through a long superconducting tube with thick walls. The fields due to these currents will induce a supercurrent I in the walls of the tube whose result, due to the Meissner effect, is to null the net flux in the tube, and is thus

of magnitude $I = -(I_1 + I_2)$. The current I flowing in the outside wall of the tube will produce a field which can be detected with a SQUID, whose output can be fed back in the usual nulling way to adjust the current I_2 to make $I = 0$, at which point I_2 will exactly equal I_1. By extension, if the wires carrying I_1 and I pass through the tube N_1 and N_2 times respectively, we will have $I = -(N_1 I_1 + N_2 I_2)$, so that at null $I_2 = (N_1/N_2) I_1$.

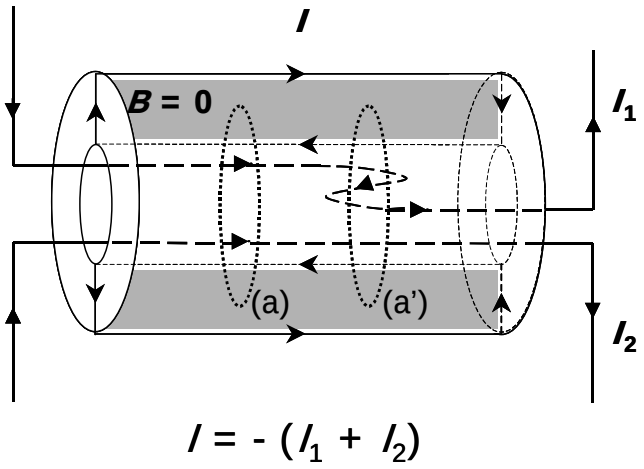

Fig. 11. Principle of the CCC. Courtesy of F. Piquémal, LNE.

The CCC was considerably advanced by the introduction of the Type II version [126]. With this device, high currents (up to 100A) can be measured by positioning the wires carrying them well away from the superconducting body of the comparator, ensuring that its critical field is not exceeded. The SQUID, measuring the current I which is to be nulled can in turn also be remote from the comparator and screened within it own superconducting shield.

Major improvements in low-T_c CCCs have recently been made by the group of Piquémal at LNE. With an $N_2 : N_1$ winding ratio of 10000:1, and very careful screening, they achieved a highly sensitive current amplifier with a noise of only $4 fA/Hz^{-½}$. It has been used in a number of high accuracy metrological applications. One is to measure the current delivered by a single-electron tunneling pump, fabricated at PTB. Current steps of few pA, with an uncertainty of a few ppm, have been observed [127].

Low-T_c CCCs have been used in association with Josephson voltage standards in resistance bridges, allowing the precise determination of voltages scaled up from the few millivolts characteristic of Josephson junctions to as much as 10V, which is much more useful to a calibration engineer [128]. They have also been used directly in resistance bridges, allowing standard wire-wound resistors to be calibrated against quantum Hall resistance standards [129]. In addition they have also been used as ultralow current amplifiers: sensitivities down to 80 $aA/Hz^{½}$ were achieved at NPL, and this has been extended to the direct sensing of charged particle beams [130]. Here I_1 is produced by the current in a high energy accelerator or ion implantation system.

Another use for ultralow current sensitivity CCCs has been in measuring the capabilities of single-electron-tunneling devices [SET] [131, 132], where currents tend to be on the order of 10-100 pA and less. In the standards community, the ultimate aim is the closure of the *quantum metrological triangle*. The aim is to relate the quantities obtained from the three quantum based phenomena, namely the Quantum Hall Effect (Resistance - the Ohm), Josephson frequency relation (Voltage - the Volt) and SET/Coulomb blockade (Current - the

Ampere). These are believed to provide the values of h/e^2, $2e/h$ and e. Measurements at the 1 part in 10^8 level are sought and the self consistency of the results will provide a fundamental test of the three underlying theories.

D. Superconducting Quantum Interference Filter

A basic dc SQUID exhibits a critical current versus field periodicity (Φ_0/AS) which corresponds to increments of one flux quantum in the loop area AS. This points to the idea that some combination of several SQUIDS with different loop areas A_{sn} might generate an oscillating field pattern with Fourier components given by the various terms Φ_0/A_{sn}. As discussed at some length in Part I, this leads to the concept of an infinite combination of all possible areas generating a field pattern which is constant everywhere apart from exhibiting a δ-function dip at $B = 0$ [133]. Though such a combination is of course impossible, it has been shown that a series combination of a large number (>~20) of SQUIDs whose individual areas are an appropriately chosen set of incommensurate values comes close to this behavior [134,135]. This makes possible the concept of identifying an applied field of precisely zero to the accuracy of the precision of typical good SQUIDs (say 10 fT). An extension of this [136] opens the possibility of magnetometers which can measure the exact value of a local field rather than just the magnitude of temporal spatial variations, a capability which would be much welcomed in several applications such as geomagnetic surveying.

G. Future prospects

Science and industry demand ever more sensitive measurements on objects in the micro- and nanoscale, as exemplified by spintronics, nanoelectromechanical systems, and spin-based quantum information processing, where single magnetic moment detection poses a grand challenge. SQUID devices with a loop size in the sub-micron range, usually called nano-SQUIDs, are currently being developed to address this issue. When fabricating those devices one faces the problem that the conventional Nb/AlOx/Nb junction technology cannot be applied because of the very small junction area required.

In the framework of the joint research project “NanoSpin”, funded by the European metrology research program, PTB in collaboration with NPL are developing nanoSQUID systems intended for the detection of single magnetic moments [137]. In first joint experiments with such a system, consisting of a nano-structured SQUID loop and a series SQUID array amplifier, a white flux noise level of 0.2 $\mu\Phi_0/\sqrt{\text{Hz}}$ could be demonstrated: this corresponds to a predicted spin sensitivity of ca. 2 units of electron spins per √Hz.

VI. USE OF SQUIDS IN FUNDAMENTAL SCIENCE

A. Introduction

We look now at a few of the ways in which SQUIDs have been applied, or proposed, as keys to the investigation of fundamental science issues, some of them, as yet, very speculative. The first involves the very basics of high-T_c superconductivity itself. Because the nature of electron pairing in the superfluid appears to involve *d*-wave atomic orbitals rather than the *s*-wave coupling found in the low-T_c materials, phase differences in the electron wave function

appear in different crystallographic directions within the superconductor. This can be exploited in bicrystal and other geometries of Josephson junction, to produce so called *π-junctions* (usually written pi) and *π-SQUIDs* which show promise for a number of novel measurement applications.

We mention in passing here that SQUIDs are at the heart of a number of schemes for developing *quantum computers*, whether as qubits in their own right or as instruments to measure the state of another quantum system such as a single spin. This is a very involved area, and we will not discuss it in detail here, because it is to be the subject of a review in a future issue of ESNF.

The attempted detection of the long postulated *gravity waves* was an area in which SQUIDs were much involved 20-30 years ago. They have given way to laser interferometers in more recent projects, but later times have seen a revival of SQUID interest, especially in Europe. Subsidiary to this has been the realization that SQUIDs could also be used in the possible detection of a dark matter particle, the *axion*, which is required by some versions of *grand universal theory.*

A SQUID use in fundamental science, which is quickly growing in importance, is the readout of arrays of sensitive electromagnetic radiation detectors used in telescopes for astrophysical studies. This topic was presented in Section III above. However, SQUIDs fabricated with loop dimensions in the submicron or even nanometer range (nanoSQUIDs) also show promise as radiation detectors called Inductive Superconducting Transition Edge Detectors (ISTEDs), and in a new family of mechanically resonant devices, nano-electromechanical systems (NEMS), which would allow detection of very small forces and particles such as single atomic or nuclear spins, and the measurement of masses as small as those of single atoms and molecules.

B. Pi-junctions and Pi-SQUIDs

At present, pi-junctions themselves are objects of basic research rather than instrumental tools for scientific investigations. Two types of junctions involving a π phase shift across them are known [138]. The first involves including a ferromagnet layer between the tunnel barrier and one of the two superconductor layers, and relies on the spatial oscillation, and thus the phase variation, of the superconducting wave function which is induced in the oxide tunnelling layer by the proximity effect. However, we focus here on grain boundary junctions between high-T_c superconductors. Here, the coupling across the barrier involves two $d_{x^2-y^2}$ orbitals, one on each side of it. Two orthogonal orientations of the lobes of these orbitals are possible, with a relative phase difference of π radians. It is thus possible to have two different varieties of junctions, depending on the relative orientation of the crystal direction on either side of the junction: across one there will be a resting phase difference of 0 radians, while across the other it is π radians. (The same two differences can be achieved by making one of the two superconductors an *s*-wave one, such as Nb.) The effect of this is immediately seen in the magnetic field "diffraction" and "interference" effects displayed by the two versions. One type (0 radians) behaves conventionally, but in the second, because the included π difference is equivalent a $\frac{1}{2}\Phi_0$ flux in the junction, the graphs of critical current versus applied field are appropriately displaced. More striking is the behavior of a dc SQUID configuration shown in Figure 12, in which one of the two junctions is a 0 radian type, while the other is a pi one. Since the total phase difference around the loop is constrained to be 2π as in all closed superconducting paths, it follows that the unperturbed pi-SQUID will contain a flux of $\frac{1}{2}\Phi_0$ (semi-fluxon), and that the usual V-$\Phi_{applied}$ curve will have a zero, rather than a maximum, at –

$\Phi_{applied}$ =0, and though still periodic in Φ_0 will be displaced by ½Φ_0 relative to that of a conventional SQUID.

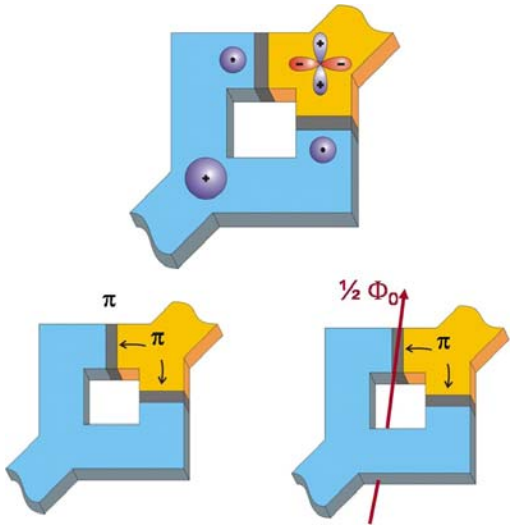

Fig. 12. Pi-ring based on the combination of a *d*-wave high-T_c superconductor and an *s*-wave low-T_c counterpart (top). In the limit of a small LI_c product the *d*-wave-induced π -phase shift is compensated by a π -phase shift enforced over one of the junctions (below left). In the limit of large LI_c values, the lowest energy state is obtained by compensating the *d*-wave-induced phase shift by a spontaneously generated half-integer flux quantum ½Φ0 (below right) [138]. Reproduced with permission (IOP).

The π shifting junctions are not only objects of fundamental research, but also represent new possibilities for superconducting electronic components and circuits, though progress is as yet in its infancy. For example, because the two lowest energy flux states of a pi-SQUID contain +½Φ_0 and -½Φ_0, it could be the basis of a bistable binary computer element. Indeed, a toggle flip-flop which might be used in an RSFQ logic circuit has recently been demonstrated [139].

C. Gravity wave and dark matter detection.

Gravity waves are predictions of the General Theory of Relativity. They are emitted during the explosion of a stellar body (*supernova)* or even during the rotation of a massive binary star pair, and in small black hole or neutron star mergers. Travelling at the speed of light, here on Earth they would produce relative distortions of the local space-time metric of order 1 in 10^{19} for events in our galaxy, and much smaller for extragalactic occurrences. Since "local" events occur only on a scale of once in a century or so, reliable detection (several events per year) has to focus on more distant events and on a metric distortion down to 1 in 10^{24}. This means that an object of physical size 1m will contract in length by 10^{-24} m, and oscillate with a period of order 1ms, for a time determined by its mechanical *Q*, assuming it is tuned to the appropriate frequency. Detection requires a method of measuring such tiny relative length contractions.

Early attempts involved the construction of highly tuned mechanical transducers, in which the tiny displacements of a massive aluminium or niobium bar were transformed by coupling it mechanically to a light *resonant* superconducting membrane, resonating at the

frequency of the large mass. This gave a mechanical displacement amplification of several orders of magnitude, which compressed the magnetic field produced by a persistent mode current circulating within a superconducting enclosure surrounding the membrane. The changed magnetic field induced a current in a SQUID pick-up coil, and the SQUID in turn provided a measurement of the amplitude of the oscillation induced in the bar (eventually, hopefully, by a passing gravitational wave). Figure 13 shows an example of such a transducer. Its analysis can be found in [140].

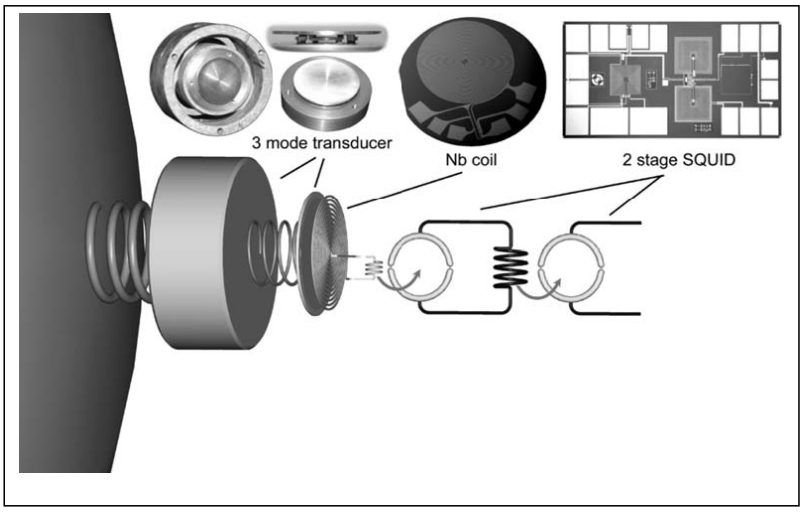

Fig. 13. Schematic view of a 3 mode inductive mechanical transducer, in this case as used on MiniGRAIL [144] (see discussion and reference to MiniGrail below). Reproduced with permission (IOP).

The technology required proved formidable. Thus it proved necessary to make the bar very highly resonant, with Q values exceeding 10^6, to cool the bar, often several tons in mass, to well below 1 K, and to develop SQUIDs with energy resolutions close to the quantum limit of order h. Though this was achieved, and metric distortions of order 1 part in 10^{-19} made practicable, no events, which require synchronous detection by a number of instruments located around the world, were reliably detected. Attention turned, and is still largely focused on, the use of long baseline (on the order of many kilometers) Michelson interferometers, in which the two (orthogonal) baselines will in general contract by different amounts much greater than those in a 1-m-long bar. Several international projects will be live soon, and there is a plan to produce a space borne system (LISA), in which the baseline is on the scale of millions of kilometers, and which should achieve sensitivities of $10^{-23}\mathrm{Hz}^{-½}$.

Lately, however, there has been renewed interest in mechanically resonant structures and SQUID detection, and three such projects are current in Europe, the NAUTILUS and EXPLORER instruments (collaborations between several institutes in Rome with EXPLORER being physically located at CERN), AURIGA (INFN, Italy), and the MINI-GRAIL instrument (universities of Leiden, Twente, and other collaborators).

NAUTILUS [141], EXPLORER, and AURIGA [142] have been running since the 1980's, though on an intermittent basis which has allowed for several successive improvements. These are aluminium bar-type devices which essentially determine one directional component of any gravitational wave pulse excitation. The bars, whose mass is of order 2300 kg, are cooled to about 2.5 K (EXPLORER - liquid helium refrigeration) and 0.1 K (NAUTILUS - dilution refrigeration) and have resonant frequencies of around 0.9 kHz. Mechanical oscillations induced by a passing gravitational pulse are amplified by ~10^4 by the coupled

membrane device discussed above. The membrane is in turn capacitively coupled to a dc SQUID and the bar excitation amplitude read out.

The SQUID science and engineering contributions to these projects have focused on mechanical designs which advance the coupling discussed earlier, on improved SQUIDs which are close to the quantum noise limits, and on lower noise readout circuitry. The best strain sensitivities achieved have been of order 10^{-20}, and in particular for NAUTILUS have been 3×10^{-20} over a bandwidth of about 25Hz around resonance, improving to 5×10^{-22} at the two resonances of the coupled oscillator system: 907 Hz and 923Hz. The designers believe that with further improvements to readout algorithms a CW gravitational signal (which might be emitted by an appropriately co-orbiting binary star combination) a strain sensitivity of 3×10^{-25} would be measurable [141].

A drawback of resonant bar systems is that they will detect only one polarization of gravitational wave, which is the one parallel to the axis of the bar. By contrast, resonant spheres have a number of advantages over bars, including the fact that they are omni-directional. MiniGRAIL is an example of such a departure in design strategies. At its heart is the structure illustrated in Figure 14, which shows a sphere made of CuAl6%, of diameter 0.65 m (much less than the length of a typical bar. and density 8000 kg m^{-3}, much higher than the Al of which bar detectors have been made [143]. The sphere has five spherical quadrupole modes of vibration, each of about 3,000Hz, and with five transducers placed at convenient positions on it, measurements of their respective amplitudes can in principle be used to determine the amplitude and polarization of the gravitational wave which excites them [144].

So far, MiniGRAIL has been operated at 5 K with three mechanical transformers, with just one coupled inductively to its own two-stage dc SQUID amplifier. A peak strain sensitivity of 1.5×10^{-20} m $Hz^{-½}$, with a value of 5×10^{-20} m $Hz^{-½}$ averaged over a bandwidth of 30Hz, have been achieved. Ultimately, with the sphere cooled by dilution refrigerator to 50mK, values over an order of magnitude superior are expected.

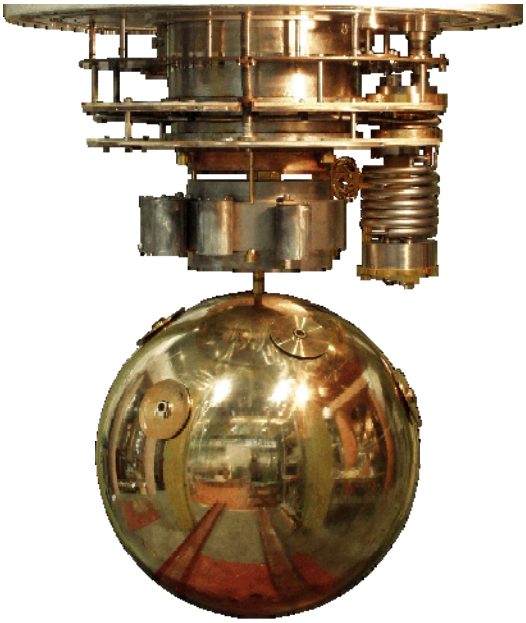

Fig. 14. The ultracryogenic spherical antenna MiniGRAIL. It will be cooled to as little as 50mK by the dilution refrigerator mounted above the CuAl6% sphere [144]. Reproduced with permission (IOP).

Interest in the gravitational wave detector has led on to the question of probing more deeply into the validity of the standard model. Initially this has been about testing the inverse square model more carefully, but it led in turn to proposals for the Satellite Test of the Equivalence Principle (of gravitational and inertial mass). This would have involved SQUID displacement sensors of the type discussed above, but appears to have been abandoned, at least for now. However interest has continued into exploring the existence of dark matter particles such as *axions*, predicted to be light mass pseudoscalar particles which mediate a very weak short range force between mass and intrinsic spin, and here SQUID science has shown that it may have a role to play. Axions would have largely decoupled from the rest of the universe shortly after the Big Bang, but in the presence of a strong magnetic field of 8T, an axion wuld be expected to undergo conversion to a real photon of energy 1 to 10 μeV, and a virtual one. The radiation might be produced in an appropriate tunable cavity resonator and detected using a cooled HEMT, but the expected levels are so low that for an appropriate cavity resonant frequency sweep (0.24 GHz to 2.4GHz), one might need several tens of years to achieve a positive result. No results have been reported as yet. However, Mück *et al.* have demonstrated a microstrip SQUID amplifier (discussed in Part I), which produced gains of 10 to 20dB at 4.2K, and pointed out that if the cavity is cooled to about 0.1K and the HEMT replaced by such an amplifier, also cooled to 0.1K, following an SIS mixer, performance would become quantum limited, and the axion detection scan reduced to a few days [145].

D. NanoSQUIDs and their Application to Extreme Sensors

NanoSQUIDs, whose early development involved Twente and NPL, have been a burgeoning area of development over the last few years, and have recently been reviewed by Foley and Hilgenkamp [146]. DC nanoSQUIDs, which are produced using nanolithography, typically consist of Dayem bridge junctions produced by focused ion beam lithography, and incorporated in loops of area 200 nm × 200 nm. They have been shown to have sensitivities as good as 0.2 $\mu\Phi_0\ Hz^{-½}$, and to have flux coupling capabilities good enough to detect single quantum spins. The application of nanoSQUIDs to the development of qubits should be covered by a future ESNF article, but here we discuss their two possible uses as extreme sensors: (i) as very sensitive radiation detectors, Inductive Superconducting Transition Edge Detectors (ISTED), sensing radiation, both electromagnetic and nuclear particle, and (b) as nanoscale electromechanical systems.

An ISTED is based on a superconducting thin film absorber and a coupled nanoSQUID, thermally biased a little below its critical temperature (where the penetration depth begins to diverge) [147], unlike a conventional transition edge detector (TES) which is biased at the steepest part of its resistive transition. When the absorber is irradiated with infrared or particles, Cooper pair breaking causes its London penetration depth to increase and to very rapidly change the inductive coupling to the SQUID producing a matching change in its output. It has been suggested that such devices will be able to detect single photons or other particles with sensitivity of 1eV and accuracy of 0.1% on a time scale of 1ns, much faster than other sensors, superconducting or otherwise.

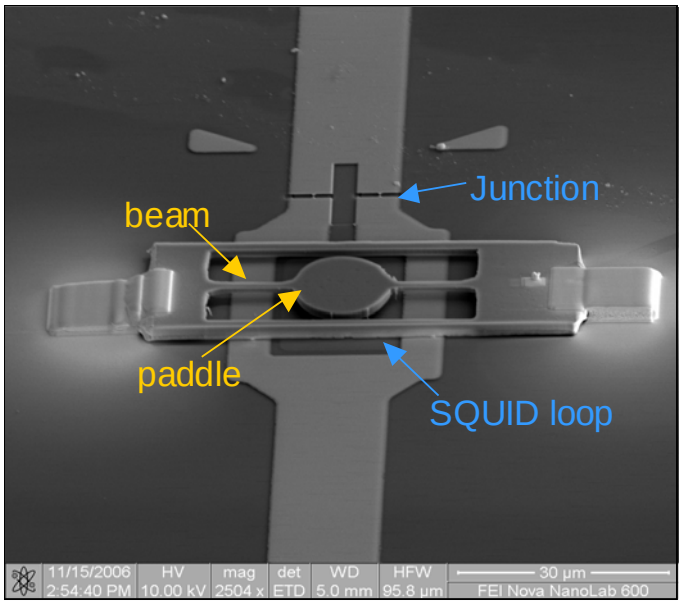

Fig. 15. SEM microphotograph of an Al-coated Si paddle NEMS resonator e-beam welded to the substrate and coupled to a nanoSQUID [148]. The cantilever beam is 1 µm wide and the paddle diameter is 15 µm. Reproduced with permission (IEEE).

Finally, we mention nanoscale electromechanical systems (NEMS). In place of the absorber, a mechanical electrically conducting resonator "paddle" in the form of a very narrow conducting beam cantilever and with a larger diameter circular paddle at its middle can be formed and fixed just above a nanoSQUID loop, as shown in Figure 15 above [148]. By passing an rf or microwave current along the beam in the presence of an orthogonal magnetic field, the Lorentz force sets the beam oscillating in the third perpendicular direction. This was modeled for a micron-scale paddle structure oscillating at between 2 and 10MHz, depending on the mode (*z*-displacement or *x*-*y* torsion). Its inductive coupling to the SQUID's sensing loop produces a corresponding signal output. If the mechanical oscillation properties of the cantilever (mean displacement, resonant frequency, *etc*.) are changed by loading it with an applied force, this will appear as sidebands. Substantial future developments of NEMS are expected, to encompass measurement methods for mass, force, charge and spin, and also single molecule biosensing and quantum information processing. Thus displacement sensitivities of $<10^{-13}$ m $Hz^{½}$ have been predicted [148], but not yet demonstrated.

H. Conclusion and Future Developments

Gravitational wave detectors of all types (interferometric, resonant bar and resonant sphere) are approaching sensitivity performances of 10^{-22}m $Hz^{-½}$ and better, at which it is predicted that several extra-galactic events per year should be observable. Whether or not they are seen, and if they are, whatever the type of instrument to detect them first, it seems likely that deployment and further development of each will continue. This is partly because true 'detection' requires coincident observation at several locations around the world, but more because the existence of gravity waves is required by the Standard Model, and if they are not found in first searches at this level, further probing at greater sensitivities will be necessary in order to investigate this model's validity, and if necessary to develop modifications to it.

Achievable sensitivities of 10^{-24} m $Hz^{-½}$ have been mentioned for mechanically resonant structures, though the proposed LISA space-borne interferometric system claims an expected performance several orders of magnitude superior to this.

Further development of nanoSQUIDS seems likely, for two principal purposes. First, their potential as readouts for ITSED radiation sensors ensures interest in their possible usefulness in instruments such as calorimeters and bolometers for detecting infrared and sub-millimeter radiation and to count individual photons from the near infrared to the X-ray range. Second, since some of the candidates for use as qubits in quantum computing involve the orientation of entities such as single ionic spins, nanoSQUIDS are being developed with the aim of detecting them. Qubits should be the topic of a future ESNF review.

VIII. PROTOTYPING AND INDUSTRIAL ACTIVITIES

Our overview of SQUID applications shows that most of these require only a limited number of highly specialized instruments or systems, even if a single system might contain a rather large number of SQUIDs, as is the case in astronomy applications. Therefore, many commissioned and successful applications are unique, custom-made systems entirely or largely constructed and fabricated by research institutions or their pilot fabrication lines. The development of such instrumentation can be viewed as modeling or prototyping. At best, limited numbers of standardized models are fabricated by small spin-off companies, usually utilizing the fabrication equipment of mother institutes. Therefore, the direct economical impact of SQUID manufacturing is minimal, even if the indirect impact could be large, as in the case of geophysical survey equipment. Of all applications reviewed, only the biomedical still holds some promise of a larger market, and even this perspective is most uncertain. It is rather difficult to predict whether standard diagnostic applications of MEG and MCG (MFI) will take off or not.

Probably the most competent worldwide manufacturer of large biomagnetic imaging systems for brain research and diagnostics is the Finnish Elekta Neuromag [20]. Two other small European companies, BMDSys (Germany) [31] and AtB (Italy) [22], also manufacture large biomagnetic imaging systems. CRYOTON (Russia) manufactures small and medium-size multichannel systems for various applications, also biomedical [149]. Other small European companies, which offer some SQUID systems in addition to SQUID components and electronics are SUPRACON, which manufactures geomagnetic systems [103], MAGNICON, which manufactures SQUID noise thermometers [150] and QEST, which develops airborne broadband antennas incorporating SQIF amplifiers [151]. What is missing on the European scene is a manufacturer of SQUID-based instruments for the measurement of magnetism and magnetic properties of matter [84]. This niche is solidly occupied by Quantum Design, Inc. (QD), a US company [152].

IX. CONCLUSIONS AND OUTLOOK

We conclude by noting that European R&D has contributed significantly to SQUID applications such as biomagnetism, NDE, geophysical surveying and metrology, while it has been lagging behind the US in large detector array SQUID readout for astrophysical cameras and spectrometers of stationary telescopes and space missions. Multiple current European activities in that domain might in the future reduce or eliminate the lag. This area is currently the fastest growing application of SQUIDs and SQIFs, and many new developments can be anticipated. In our opinion, the most notable European success of this decade has been the

development and commercial acceptance of full tensor low-T_c geophysical surveying systems. The indirect economic impact of these can be considerable. In the future, appropriate SQUID systems might also find use in hydrocarbon (oil) exploration. We also placed some emphasis on the future opportunities in science and metrology opened by nanoSQUIDs as extreme sensors; an area of vivid European activities.

In this decade, SQUIDs nearly lost their absolute primacy as the most sensitive detectors of magnetic field. The optically pumped atomic (absolute) magnetometers operating at room (in reality elevated) temperature were demonstrated with a noise floor of the same order of magnitude [153]. However, the vectorial characteristics of a SQUID detector and the fact that it is sensitive to magnetic flux (field) change rather than to its absolute value will made it hard or impossible to replace in most current applications. The recent rapid rise of SQUID arrays as the most sensitive, high-gain cryogenic current amplifiers of radiation and particle detector signals is just one more example of SQUID unique capabilities. Nevertheless, SQUIDs achieve lower flux noise, but higher field noise as they are shrunk. Should one need the lowest noise in a device with extremely small area, atomic magnetometers might do better in some applications.

In this overview, we did not discuss SQUID cooling, and the importance in many applications of replacing liquid cryogens by low-noise (and minimal maintenance) mechanical cryocoolers. While in space missions of longer duration such a cooling mode might be the only one possible, cryocooling could reduce the acceptance threshold in many application fields, especially industrial and clinical. The development of sufficiently "quiet" cryocoolers, "invisible" to the user, highly reliable and nearly maintenance-free remains the most desirable goal for the future.

ACKNOWLEDGEMENTS

We express our special gratitude to John Clarke (UC Berkeley), who reviewed manuscripts of both parts of this overview and provided most helpful critical comments, which significantly improved it. We are very indebted also to Piet de Korte (SRON) and Torsten May (IPHT-Jena) for their comments on Section III, to Cathy Foley (CSIRO) and Ronny Stolz (IPHT-Jena) for correcting Section V, and to John Gallop (NPL), François Piquémal (NLE), Thomas Schurig and Alexander Zorin (both PTB) for comments to Section VI. Furthermore, we are indebted to the following colleagues, who provided some of the figures and/or references used here: Antti Ahonen (Elekta Neuromag), Bob Fagaly (then at Tristan Technologies), Jaap Flokstra (Twente Univ.), H. Jochen Krause (FZ Jülich), Torsten May, Thomas Schurig, Ronny Stolz, Dag Winkler (Chalmers Univ.). Last, but not least, we thank Colin Pegrum (University of Strathclyde) for extended help with literature searches.

REFERENCES

[1] J. Clarke, "A superconducting galvanometer employing Josephson junction", *Phil. Mag*. **13**, 115 (1966).
[2] J. Clarke, „Measurement of small voltages using a quantum interference device", in *Proc. on the Physics of Superconducting Devices*, B.S. Deaver, Jr., and W.S. Goree (Eds), Univ. of Virginia, Charlottesville (1967).
[3] J. Clarke, Doctoral Dissertation (1968), private communication (unpublished).
[4] J. Clarke and A.I. Braginski (Eds.), *The SQUID Handbook,* , Wiley-VCH, Weinheim, vol. II (2006).
[5] A.I. Braginski, G.B. Donaldson, "SQUID Activities in Europe, Part I: Devices"; ESNF, No. 8, CR12-I (2009).

[6] J. Vrba, J. Nenonen, L. Trahms, "Biomagnetism" in *The SQUID Handbook,* J. Clarke and A.I. Braginski (Eds.), Wiley-VCH, Weinheim, vol. II (2006), pp. 269-389.
[7] W. Andrä and H. Nowak (Eds.), *Magnetism in Medicine,* 2nd Edition, Wiley-VCH, Weinheim 2006.
[8] K. Sternickel, A.I. Braginski, "Biomagnetism using SQUIDs: status and perspectives", *Supercond. Sci. Technol*. **19**, S160 (2006); the list of all biomagnetic apptications from this reference is provided here.
[9] D. Cohen, E.A. Edelsack, J.E. Zimmerman, „Magnetocardiogramms taken inside a shielded room with a superconducting point-contact magnetometer", *Appl. Phys. Lett*. 16, 278 (1970).
[10] D. Cohen, "Magnetoencephalography: detection of the brain's electrical activity with a superconducting magnetometer", *Science*, 175, 664 (1972).
[11] R. Ilmoniemi, R. Hari, K. Reinikainen, "A four-channel SQUID magnetometer for brain research", *Electroenceph. Clin. Neurophysiol*. **58**, 467 (1984).
[12] J.M. Jaycox, M.B. Ketchen, " Planar coupling scheme for ultra low noise dc SQUIDs", *IEEE Trans. Magn*. **MAG-17**, 400 (1981).
[13] J. Knuutila, S. Ahlfors, A. Ahonen *et al*., "Large-area low-noise seven-channel dc SQUID magnetometer for brain research", *Rev. Sci. Instr*. **58**, 2145 (1987).
[14] H.E. Hoenig, "SQUID arrays for biomagnetic diagnosis", *Physica Scripta* **T35**, 177 (1991); http://www.iop.org/EJ/article/1402-4896/1991/T35/038/physscr1_T35_038.pdf?request-id=aef6ada3-0504-408d-b213-29727da2dfb8.
[15] A.I. Ahonen, M. Hämäläinen, M. J. Kajola *et al*., "122-Channel SQUID Instrument for Investigating the Magnetic Signals from the Human Brain", Physica Scripta **T49**, 198-205 (1993).
[16] P. Laine P, M. Hämäläinen, A. Ahonen, "Combination of magnetometers and planar gradiometers in an MEG system", in *Recent Advances in Biomagnetism: Proc. 11th Int. Conf. on Biomagnetism*, T. Yoshimoto *et al.* (Eds), Tohoku University Press, Sendai (1999) pp 47-50.
[17] H. Seppä, "DC SQUID electronics based on adaptive noise cancellation and a high open-loop gain controller". In *Superconducting Devices and their Applications,* H. Koch and H. Lübbig (Eds.), Springer-Verlag, Berlin 2002, p. 346.
[18] H. Seppä, A. Ahonen, J. Knuutila *et al*., „Dc SQUID electronics based on adaptive positive feedback: experiments", *IEEE Trans. Magn*. **27**, 2488 (1991).
[19] J. Nenonen, M. Kajola J. Simola, A. Ahonen , "Total information of multichannel MEG sensor arrays", in *Biomag 2004: Proc. 14th Int. Conf. on Biomagnetism* , E Halgren *et al.* (Eds.), Biomag 2004 Inc., Boston (2004) pp 630-1.
[20] Elekta Neuromag, Siltasaarenkatu18 - 20 A, Helsinki, Finland; Mailing address: P.O. Box 68, FIN-00511 Helsinki, Finland; http://www.elekta.com/healthcare_international_elekta_neuromag.php.
[21] F. Thiel, A. Schnabel, S. Knappe-Grüneberg *et al*, „The 304 SQUIDs vector magnetometer system for biomagnetic measurements in the Berlin shielded room 2", *Biomed. Tech. (Biomedical Engineering)* **50**, 69 (2005).
[22] Advanced Technologies Biomagnetics (AtB), Via Martiri di Pietransieri 2, 65129 Pescara, Italy; http://www.atb-pro.de/company/index.php.
[23] B. Hilgenfeld, J. Haueisen, "Simultaneous suppression of disturbing fields and localization of magnetic markers by means of multipole expansion", *BioMagnetic Research and Technology* **2**, 6, 2004.
[24] M. Burghoff , T.H. Sander, A. Schnabel , *et al.* , "Dc magnetoencephalography: direct measurement in a magnetically extremely well-shielded room. *Appl. Phys. Lett* . **85**, 6278-6280 (2004).
[25] C.M. Arturi, L. Di Rienzo, J. Haueisen, "Information content in single-component versus three-component cardiomagnetic fields", *IEEE Trans. Magn*. **40**, 631 (2004).
[26] L. Di Rienzo, J. Haueisen, C.M. Arturi," "Three component magnetic field data impact on minimum norm solutions in a biomedical application", *COMPEL* **24**, 869 (2005).
[27] E.A. Lima, A. Irimia, J.P. Wikswo, "The Magnetic Inverse Problem", in *The SQUID Handbook*, J. Clarke and A.I. Braginski (Eds.), Wiley-VCH, Weinheim, vol. II, (2006), pp. 139-267.
[28] J. Clarke, M. Hatridge, M. Moessle, "SQUID-Detected Magnetic Resonance Imaging in Microtesla Fields", *Ann. Rev. Biomed. Eng*. **9**, 389-413 (2007), and references therein.
[29] European Project MEGMRI – Developing a Hybrid MEG-MRI System (2008): https://wiki.tkk.fi/display/megmri/MEGMRI;jsessionid=ECD9DD858F7579FBF0F8D4E6629A92D3.
[30] V.S. Zotev, P.L. Volegov, A.N. Matlashov, M.A. Espy, J.C. Mosher, R.H. Kraus Jr., „Parallel MRI at microtesla fields", *J. Magn. Resonance* **192**, 197 (2008).
[31] BMDSys, GmbH, Wildenbruchstr. 15, D-07745 Jena, Germany; http://www.bmdsys.com/index.php/de_DE/technology.
[32] CardioMag Imaging, Inc, http://www.cardiomag.com/.
[33] J.-W. Park, P.M. Hill, N. Chung, *et al*., "Magnetocardiography predicts coronary artery disease in patients

with acute chest pain", *Ann. Noninv. Electrocardiol*. **10**, 312 (2005).
[34] J.-W. Park, B. Leithäuser, P. Hill, F. Jung, „Resting magnetocardiography predicts 3-year mortality..", *Ann. Noninv. Electrocardiol*. **13**, 171 (2008).
[35] 1st International Perinatal Biomagnetism Workshop, http://pb2009.udanet.it.
[36] R. Fischer and D.E. Farrell, "Liver Iron Susceptometry" in Magnetism in Medicine, W. Andrä and H. Nowak (Eds.), 2nd Edition, Wiley-VCH, Weinheim 2006, pp. 529-545.
[37] G.M. Brittenham, D.F. Farrell, J.W. Harris, *et al*., *New England J. Med*. **307**, 1671 (1982).
[38] Tristan Technologies, Inc., 6185 Cornerstone Court East, Suite 106, San Diego, CA 92121 USA; http://www.tristantech.com/.
[39] D.N. Paulson, R.I. Fagaly, R.M. Touissant, R. Fisher, "Biomagnetic susceptometer with SQUID instrumentation", *IEEE Trans. Magn*. **27**, 3249 (1991).
[40] J. Clarke, A.I. Lee, M. Mück, P.L. Richards, "SQUID Voltmeters and Amplifiers", in *The SQUID Handbook*, J. Clarke and A.I. Braginski (Eds.), Wiley-VCH, Weinheim, vol. II, (2006), pp. 1-137.
[41] H.C. Seton, D.M. Bussel, J.M.S. Hutchison *et al*., "DC SQUID based NMR detection from room temperature samples", *Phys. Med. Biol*. **37**, 2133 (1992).
[42] H.C. Seton, J.M.S. Hutchison, D.M. Bussel, " A 4.2-K receiver coil and SQUID amplifier used to improve the SNR of low-field magnetic resonance images of the human arm", *Meas. Sci. Technol*. **8**, 198 (1997) and references therein..
[43] M. Burghoff, S. Hartwig, L. Trahms, J. Bernarding, "Nuclear magnetic resonance in the nanoTesla range", *Appl. Phys. Lett*. **87**, 054103 (2005).
[44] L. Qiu, Y. Zhang, H.-J. Krause *et al*., „Nuclear magnetic resonance on the earth's magnetic field using a nitrogen-cooled SQUID", *Appl. Phys. Lett*. **91**, 072505 (2007).
[45] C. Hollerith, D. Wernicke, M. Bühler, *et al*., "Energy dispersive X-ray spectroscopy with microcalorimeters", *Nucl. Instrum. Meth.* **A 520**, 606 (2004).
[46] May, G. Zieger, S. Anders, *et al*., "Passive stand-off terahertz imaging with 1 hertz frame rate" in *Terahertz for Military and Security Applications VI*, J.O. Jensen, H.-L. Cui, D.L. Woolard, R.J. Hwu (eds), *Proceedings of SPIE* **6949**, 69490C (2008).
[47] M. Kiviranta, "Use of SiGe bipolar transistors for cryogenic readout of SQUIDs", *Supercond. Sci. Technol*. **19**, 1297 (2006).
[48] M. Kiviranta, "High dynamic range SQUID readout for frequency-domain multiplexers", *J. Low Temp. Phys.* **151**, 952 (2008).
[49] D. Drung, J. Beyer, M. Peters, J. Storm, T. Schurig, "Novel SQUID current sensors with high linearity at high frequencies", *IEEE Trans. Appl. Supercond*. 19, No. 3 in press (2009).
[50] P. de Korte, J. Anquita, F. Bakker *et al*., EURECA: „European-Japanese microcalorimeter array", *J. Low Temp. Phys.* **151**, 733 (2008).
[51] T.M. Lanting, H.-M. Cho, J. Clarke *et al*., "Frequency-domain multiplexed readout of TES arrays with a superconducting quantum interference device", *Appl. Phys. Lett*. **86**, 112511 (2005).
[52] T. May *et al*., "The 350 Micrometer Wavelength Superconducting Bolometer Camera for APEX", ESNF, No. 8, ST113 (2009).
[53] F. Voisin, E. Bréelle, M. Piat *et al*., "Very low noise multiplexing with SQUIDs and SiGe heterojunction bipolar transistors for readout of large superconducting bolometer arrays", *J. Low Temp. Phys.* **151**, 1028 (2008).
[54] J. Beyer, D. Drung, M. Peters *et al*., "A single-stage SQUID multiplexer for TES array readout", *IEEE Trans. Appl. Supercond*. **19**, No. 3 in press (2009).
[55] R. Vaccarone, F. Strata, F. Gatti *et al*., "The design of a frequency multiplexed Ir-Au TES array", *J. Low Temp. Phys.* **151**, 921 (2008).
[56] R. Vaccarone, "An Analysis of Stability in Frequency Multiplexed TES Arrays",*J. Low Temp. Phys.* **151**, 15 (2008).
[57] J.A.B. Mates, G.C. Hilton, K.D. Irvin *et al*., "Demonstration of a multiplexer of dissipationless superconducting quantum interference devices", *Appl. Phys. Lett*. **92**, 023514 (2008).
[58] A.L. Woodcraft, P.A.R.Ade, D. Bintley *et al*., "Electrical and optical measurements on the first SCUBA-2 prototype 1280 pixel submillimeter superconducting bolometer array", *Rev. Sci. Instr*. **78**, 024502 (2007).
[59] J. Mehl, P.A.P. Ade, K. Basu *et al.*, "TES bolometer array for the APEX-SZ camera",*J. Low Temp. Phys.***151**, 697 (2008).
[60] N.W. Halverson, T.M. Lanting, P.A.P. Ade *et al*, "Sunyaev-Zel'dovich effect observations of the bullet cluster (1E 0657-56) with APEX-SZ, http://adsabs.harvard.edu/abs/2008arXiv0807.4208H.

[61] M.D. Niemack, Y. Zhao, E. Wollack *et al*., „A Kilopixel Array of TES Bolometers for ACT: "Development, Testing, and First Light"*J. Low Temp. Phys.* **151**, 690 (2008).
[62] Ph. Mauskopf , D. Morozov, D. Głowacka, *et al*., "Development of transition-edge superconducting bolometers for the SAFARI far-IR instrument on the SPICA space-borne telescope", *Proceedings SPIE* 7020, 70200N (2008).
[63] B-Pol Proposal, http://www.b-pol.org/index.php.
[64] M.D. Audley, D.M. Glowacka, D.J. Goldie, "Tests of finline-coupled TES bolometers for CLOVER", *Proceedings of Infrared and Millimeter Waves, 2007 and the 2007 15th International Conference on Terahertz Electronics*. *IRMMW-THz. Joint 32nd International Conference* (2007) pp.180 –181.
[65] E. Andreotti, C. Arnaboldi, P. de Bernardis, *et al*., "Mare, Microcalorimeter arrays for a Rhenium experiment: a detector overview", *Nucl. Instrum. Methods* **A 572**, 208 (2007).
[66] P. Christ, S. Rutzinger, W. Seidel *et al*., High detection sensitivity achieved with cryogenic detectors in combination with matrix-assisted laser desorption/ionisation time-of-flight mass spectroscopy", *Eur. J. Mass Spectrom*. **10**, 469 (2004).
[67] R.J.P. Bain, G.B. Donaldson, S. Evanson *et al.*. " SQUID gradiometric detection of defects in ferromagnetic structures", in H.D. Hahlbohm and H Lübbig (Eds.) *SQUID'85*, *Proc. 3rd International Conference on Superconducting Quantum Devices*, deGruyter, Berlin, (1985) pp. 841-846.
[68] H. Weinstock, M. Nisenoff, "Nondestructive evaluation of metallic structures using a SQUID gradiometer", in H.D. Hahlbohm and H. Lübbig (Eds.) *SQUID'85, Proc. 3rd International Conference on Superconducting Quantum Devices*, deGruyter, Berlin, pp. 853-858.
[69] Y. Zhang, Y. Tavrin,, H.J. Krause *et al., «* Applications of high-temperature SQUIDs" *Applied Superconductivity* **148**, 367 (1995).
[70] D.M. McKirdy, A. Cochran, A.. McNab. *et al*., "Using SQUIDs to solve some current problems in eddy current testing", *Applied Superconductivity*, **148**,. 1515 (1995).
[71] M. von Kreutzbruck, M. Muck, U. Baby *et al.*, "Experiments on eddy current NDE with HTS RF SQUIDs" *Non-Linear Electromagnetic Systems* **13**, 165 (1998).
[72] A. Barone, G Peluso, G. Pepe, *et al.*, "Design of a NDE instrumentation prototype with high-temperature SQUIDs" *Nuovo Cimento* D, **19**, 1495 (1997).
[73] P. Seidel, F. Schmidl, C. Becker *et al,*. "Planar high-temperature superconducting dc-SQUID gradiometers for different applications ", *Supercond. Sci. Technol.* **19**, S143 (2006).
[74] M.E.Walker, H. Nakane, A. Cochran *et al., "*Unshielded use of thin-film Nb dc superconducting quantum interference devices and integrated asymmetric gradiometers for nondestructive evaluation, *Appl. Phys. Lett*. **71**, 131 (1997).
[75] S. Keenan, E.J.Romans, G.B. Donaldson, "HTS SQUID NDE of curved surfaces using background field cancellation techniques", *IEEE Trans. Appl. Supercond*. **17**, 784 (2007).
[76] G. Sawade, U. Gampe. and H-J. Krause,," Non destructive examination of prestressed tendons by the magnetic stray field method", in *Proc. 4th Conf. on Engineering Structural Integrity Assessment*, J.H. Edwards *et al.* (Eds,)*.,* Cambridge, U.K., (1998) pp. 353-363.
[77] Y. Tavrin, M. Siegel, J.H. Hinken, "Standard method for detection of magnetic defects in aircraft engine discs using a HTS SQUID gradiometer", *IEEE Trans. Appl. Supercond*. **9**, 3809 (1999).
[78] A. Haller, Y. Tavrin, H-J. Krause *et al*., "Eddy current tomography using rotating magnetic fields for deep SQUID NDE", *Supercond. Sci. Technol*.. **10**, 901 (1997).
[79] K. Allweins, G. Gierelt, H.-J. Krause *et al.,* "Defect detection in thick aircraft samples based on HTS SQUID-magnetometry and pattern recognition", *IEEE Trans. Appl. Supercond*. **13**, 250 (2003).
[80] M. von Kreutzbruck, M. Mück. C. Heiden, "Nondestructive testing of aircraft parts by SQUID based eddy current systems", in *Studies in Applied Electromagnetics and Mechanics*, P. Di Barba, A. Savini (Eds.), Vol. 18, IOS Press, Amsterdam (1999), pp. 257-260.
[81] M. Mück, C. Welzel, F. Gruhl *et al.,"* Non-destructive testing of niobium sheets for superconducting resonators using an LTS SQUID system", Physica C **368**, 96 (2002).
[82] C. Bonavolonta, G.P. Pepe, G. Peluso *et al.,* "Electromagnetic non-destructive evaluation of Fiberglass/Aluminum Laminates using HTS SQUID magnetometers", *IEEE Trans. Appl. Supercond*. **15**, 711(2005).
[83] D. Graham, P. Maas, G.B. Donaldson *et al.,* "Impact damage detection in carbon fibre composites using HTS SQUIDs and neural networks", *NDT & E International* **37**, 565 (2004).
[84] R.C. Black, F.C. Wellstood, "Measurement of magnetism and magnetic properties of matter", in *The SQUID Handbook,* J. Clarke and A.I. Braginski (Eds.), Wiley-VCH, Weinheim, vol. II,(2006) pp. 391-440.
[85] M. Mück, "SQUIDs: microscopes and nondestructive evaluation", *Physic Status Solidi C.- Conferences and Critical Reviews*, **2,** 1510 (2005).

[86] I.A .Krauss, S.I, Woods and A. Orosco, "Current imaging using magnetic field sensors", *Microelectronics Failure Analysis- Desk Reference 5th Edition,* ASM Materials Park, (OH), (2004), pp. 304-312.
[87] F.C. Wellstood; J. Matthews and S. Chatraphorn, "Ultimate limits to magnetic imaging", *IEEE Trans. Appl. Supercond.,* **13,** 258 (2003).
[88] P. Pitzius, V. Dworak, U. Hartmann, "Ultra-high resolution scanning SQUID microscopy", *6th Int . Supercond. Electronics Conf. (ISEC '97) Extended Abstracts*, **3** 395 (2004).
[89] M. Adamo, C. Nappi, E. Sarnelli, "Magnetic dipole imaging by a scanning magnetic microscope", *Measurement Science & Technology*, **19**. 015508 (2008).
[90] I.A. Volkov, M.L. Chukharkin, O.V. Snigirev *et al.,*. "HTS SQUID microscopy for measuring the magnetization relaxation of magnetic nanoparticles", *IEEE Trans. Appl. Supercond*., **15** 3874 (2005).
[91] H-J.Krause, G.I. Panaitov, Y. Zhang, "Conductivity tomography for non-destructive evaluation using pulsed eddy current with HTS SQUID magnetometer ", *IEEE Trans. Appl. Supercond.* **13**, 215 (2003).
[92] J. Beyer,T. Schurig, A. Ludge, H. Riemann, " SQUID-NDE of semiconductor samples with high spatial resolution", Supercond. Sci. Technol. **13**, 532-536 (2000).
[93] C. Carr, J.C. Macfarlane, G.B. Donaldson, "A fully portable, cryocooler-based HTS SQUID NDE instrument", *IEEE Trans. Appl. Supercond*., **13,** 245 (2003).
[94] T.D. Gamble, W.M. Goubau, J. Clarke, "Magnetotellurics with a remote reference", *Geophysics* **44**, 53 (1979).
[95] J. Clarke, "Geophysical applications of SQUID", *IEEE Trans Magn*. **19**, 288 (1983).
[96] T.R. Clem, C.P. Foley, M.N. Keene, "SQUIDs for geophysical survey and magnetic anomaly detection", in *The SQUID Handbook*, J. Clarke and A.I. Braginski (Eds.), Wiley-VCH, Weinheim, vol. II, (2006), pp. 481-543.
[97] K. E. Leslie, R. A. Binks, S. K. H. Lam, *et al*., "Application of high-temperature superconductor SQUIDs for ground-based TEM", *The Leading Edge* **27**, 70 (2008).
[98] C.P. Foley, K.E. Leslie, R.A. Binks, "A history of the CSIRO's development of high temperature superconducting rf SQUIDs for TEM prospecting", *First Break* **25**, 73 (2007).
[99] C.P. Foley, D.L. Tilbrook, K.E. Leslie *et al*., "Geophysical exploration using magnetic gradiometry based on HTS SQUIDs", *IEEE Trans. Appl. Supercond*. **11**, 1375 (2001).
[100] Leslie, K.E. Binks, R.A. Foley *et al*., "Operation of a geophysical HTS SQUID system in sub-Arctic environments", *IEEE Trans. Appl. Supercond*. **13**, 759 (2003).
[101] V. Zakosarenko, A. Chwala, J. Ramos *et al*.,"HTS dc SQUID systems for geophysical prospection",*IEEE Trans. Appl. Supercond*. **11**, 896 (2001).
[102] A. Chwala, V. Schultze, R. Stolz *et al*., „An HTS dc SQUID system in competition with induction coils for TEM applications", *Physica* C **354**, 45 (2001).
[103] SUPRACON, AG, Wildenbruchstr.15, D-07745 Jena, Germany; www.supracon.com.
[104] C. Foley (CSIRO); private information (unpublished), July 2009.
[105] Spectrem Air, 23 Somewhere Str., Durban 1234, South Africa; www.spectrem.co.za.
[106] Geotech Ltd., 245 Industrial Parkway North Aurora, Ontario L4G 4C4, Canada; www.geotech.ca.
[107] J.B. Lee, D.L. Dart, RJ. Turner *et al*., "Airborne TEM surveying with a SQUID magnetometer sensor", *Geophysics* **67**, 468 (2002).
[108] P.W. Schmidt, D.A. Clark, "Advantages of measuring the magnetic gradient tensor", *Preview* **84**, 26 (2000).
[109] R. Stolz, L. Fritzch, H.-G. Meyer, "LTS SQUID sensor with a new configuration", *Supercond. Sci. Technol*. **12**, 806 (1999).
[110] K.P. Humphrey, T.J. Horton, M.N. Keene, "Detection of mobile targets from a moving platform using an actively shielded, adaptively balanced SQUID gradiometer.", *IEEE Trans. Appl. Supercond*. **15**, 753 (2005).
[111] H.-G. Meyer, R. Stolz, A. Chwala, M. Schulz, "SQUID technology for geophysical exploration", *Phys. Stat. Sol*. (c) **2**, 1504 (2005).
[112] S. Linzen, V. Schultze, A. Chwala *et al*., "Quantum Detection Meets Archaeology – Magnetic Prospection with SQUIDs, Highly Sensitive and Fast", in New Technologies for Archeology, M. Reindel and G.A. Wagner (Eds.), Springer-Verlag, Berlin & Heidelberg (2009), pp. 71-85 and 465-504.
[113] G. Waysand, P. Barroy, R. Blancon *et al*., "Seismo-ionosphere detection by underground SQUID in low-noise environment in LSBB-Rustrel, France", *Eur. Phys. J. Appl. Phys*. **47**, 12705 (2009).
[114] A.C. Fraser-Smith, A. Bernardi, P.R. McGill *et al*., "Low-frequency magnetic field measurements near the epicenter of the Ms 7.1 Loma Prieta Earthquake", *Geophys. Res. Lett*. **17**, 1465 (1990).
[115] Y. Machitani, N. Kasai, Y. Fujinawa *et al*., "Vector HTS-SQUID system for ULF magnetic field monitoring", *IEEE Trans. Appl. Supercond*. **13**, 763 (2003).
[116] P. Schmidt, D. Clark, K. Leslie *et al*., "GETMAG: a SQUID magnetic tensor gradiometer", *Explor.*

Geophys. 35, 297 (2004).
[117] D.L. Tilbrook, "Rotating magnetic tensor gradiometry and a superconducting implementation", *Supercond. Sci. Technol*. **22**, 075002 (2008).
[118] J. Gallop, F. Piquémal, "SQUIDs for standards and metrology", in *The SQUID Handbook,* J. Clarke and A.I. Braginski (Eds.), Wiley-VCH, Weinheim, vol. II, (2006), pp. 481-543.
[119] S. Menkel, D. Drung, Ya.S. Greenberg, Th. Schurig, "Integrated thin-film dc RSQUIDs for noise thermometry", *J. Low. Temp. Phys*. **120**, 381 (2000).
[120] J. Beyer, D. Drung, A. Kirste, *et al.*, "A magnetic-field-fluctuation thermometer for the mK range based on SQUID magnetometry", *,IEEE Trans. Appl. Supercond*. **17**, 760 (2007).
[121] C.P Lusher, J. Li, V.A. Maidanov et al., "Current sensing noise thermometry using a low Tc DC SQUID preamplifier", *Meas. Sci. Technol*. **12** 1 (2001).
[122] J. Engert, J. Beyer, D. Drung *et al*., "Practical noise thermometers for low temperatures", *J.Phys. Conf. Ser.,* **150**, 012012 (2009).
[123] L. Hao, J.C. Gallop, R.P. Reed *et al*., "HTS SQUID application as a quantum roulette noise thermometer", *IEEE Transactions on Applied Supercond.* **9**, 2971 (1999).
[124] C.H. Gardiner, R.A.M. Lee, J.C. Gallop *et al*., "Degenerate ground state and anomalous flux hysteresis in a $YBa_2Cu_3O_7$ grain boundary rf SQUID", *Supercond. Sci. Technol*. **17** S234 (2004).
[125] J.M. Williams, P. Kleinschmidt, "A cryogenic comparator bridge for resistance measurements at currents up to 100A", *IEEE Trans. Instrum. Meas.,* **48**, 375 (1999).
[126] F. Gay, F. Piquémal, G. Geneves, "Ultralow noise current amplifier based on a cryogenic current comparator", *Rev. Sci. Instrum*. **71**, 4592 (2000).
[127] B. Steck, A. Gonzalez-Cano, N. Feltin N *et al.*, "Characterization and metrological investigation of an R-pump with driving frequencies up to 100 MHz", *Metrologia*, **45**, 482-491, (2008).
[128] A. Cerrudo, J. Sese, L. Gomez *et al*., "Semi automated dc-SQUID based CCC bridge for precision resistance measurements at the Spanish TPYCEA (2008)", *2008 Conference On Precision Electromagnetic Measurements Digest*, pp. 154-155.
[129] F. Raso, R. Hernandez, A. Mendez *et al*., "Proposal of a new method of measurement of the quantized Hall resistance with a binary Josephson array in a bridge configuration", *2008 Conference On Precision Electromagnetic Measurements Digest,* pp. 162-163.
[130] L. Hao, J.C. Gallop, J.C. Macfarlane, C. Carr, "HTS cryogenic current comparator for non-invasive sensing of charged particle beams", *IEEE Trans. Instrum. Meas*., **52** 617 (2003).
[131] N. Feltin, L. Devoille, F. L., Piquémal, *et al*., "Progress in measurements of a single-electron pump by means of a CCC", *IEEE Trans. Instrum. Meas*., **52** 599-603 (2003).
[132] B. Steck, A. Gonzalez-Cano, N. Feltin, *et al.*, "Characterization and metrological investigation of an R-pump with driving frequencies up to 100MHz", *Metrologia* **45**, 482 (2008).
[133] P. Carelli, M.G. Castellano, K. Flacco et al., "An absolute magnetometer based on dc superconducting quantum interference devices", *Europhys. Lett*. **39**, 569 (1997).
[134] J. Oppenländer, Ch. Häussler and N. Schopohl, Non-Φ_0-periodic macroscopic quantum interference in one-dimensional parallel junction arrays with unconventional grating structure, *Phys. Rev*. **B 63**, 024511 (2000).
[135] J. Oppenländer, Ch. Häussler and N. Schopohl, "Nonperiodic flux-to-voltage conversion of series arrays of dc superconducting quantum interference devices", *J. Appl. Phys*. **89**, 1875 (2001).
[136] P. Caputo, J. Tomes, J. Oppenlander *et al.*, Superconducting quantum interference filters as absolute magnetic field sensors, *IEEE Trans. Appl. Supercond*., **15**, 1044 (2005).
[137] Project T4.J02, "Nanomagnetism and Spintronics", www.nanospin.eu.
[138] H. Hilgenkamp Pi-phase shift Josephson structures, *Supercond. Sci. Technol*. **21** 034011. (2008).
[139] T. Ortlepp, Ariando, O..Meike et al., "Flip-Flopping Fractional Flux Quanta", *Science*, 312, 1495 (2006).
[140] Ho Jung Paik, "Gravity and Motion Sensors", in *The SQUID Handbook,* J. Clarke and A.I. Braginski (Eds.), Wiley-VCH, Weinheim, vol. II,(2006) pp. 545-579.
[141] P Astone, D Babusci, M Bassan *et al.*, "The next run of the gravitational wave detector NAUTILUS", *Class. Quantum. Grav.*, **19** 1911 (2002).
[142] L.Baggio, M.Bignotto, M.Bonaldi*et al.*, "3-Mode detection for widening the bandwidth of resonant gravitational wave detectors", *Phys. Rev. Lett*. **94** 241101 (2005).
[143] A de Waard, L Gottardi, J van Houwelingen *et al.* "MiniGRAIL, the first spherical detector", *Class. Quantum. Grav.*, **28** S143-S151 (2002).
[144] J Pleikies, O. Usenko, H.E. Kuit *et al*., "SQUID developments for the gravitational antenna MiniGRAIL", *IEEE Trans. Appl. Supercon,* **17** 764 (2007).
[145] M, Muck, C. Welzel, J. Clarke, "Superconducting quantum interference device amplifiers at gigahertz

frequencies", *Appl. Phys. Lett*., **82**. 3266 (2003).
[146] C.P. Foley and H. Hilgenkamp, "Why nanoSQUIDs are important; an introduction to the focus issue", *Supercond. Sci. Technol*. **22** 064001 (2009).
[147] L. Hao, J.C. Macfarlane, P. Josephs-Franks*, et al*., "Inductive Superconducting transition edge photon and particle detector", *IEEE Trans. Appl. Supercond.* **16** 1479-1482 (2003).
[148] L. Hao, J.C. Gallop and D. Cox *et al.*, "Focussed Ion Beam NanoSQUIDs as Novel NEMS Resonator Readouts", *IEEE Trans. Appl. Supercond.* **19** 693-696 (2009).
[149] CRYOTON Co., Ltd, Oktjabrskiy prospect, 15-29, 142190, Troitsk, Moscow Region, Russia; www.cryoton.webzone.ru.
[150] MAGNICON, GbR, Lemsahler Landstr. 171, 22397 Hamburg, Germany; http://www.magnicon.com/squid- electronics/.
[151] QEST, Quantenelektronische Systeme GmbH, Max-Eyth-Str. 38, 71088 Holzgerlingen, Germany; http://www.qest.de/index.html.
[152] 6325 Lusk Blvd., San Diego, CA 92121-3733, USA; http://www.qdusa.com/index.html.
[153] I.K. Kominis, T.W. Kornack, J.C. Alfred, M.V. Romalis, "A subfemtotesla magnetometer", *Nature* **422**, 596 (2003).